Continuum Mech. Thermodyn. (2020) 32:987–1010
https://doi.org/10.1007/s00161-019-00804-z

ORIGINAL ARTICLE

P. Vaitheeswaran · A. Udupa · S. Sadasiva · G. Subbarayan

Interface balance laws, phase growth and nucleation conditions for multiphase solids with inhomogeneous surface stress

Received: 13 December 2018 / Accepted: 7 June 2019 / Published online: 20 June 2019

Abstract In this paper, the thermodynamic configurational force associated with a moving interface is used to derive the conditions for phase growth and nucleation in bodies with multiple diffusing species and arbitrary surface stress at the phase interface. First, the mass, momentum and energy balances are derived on the evolving phase interface. The thermodynamic conditions that result from free energy inequality at the interface are derived leading to the analytical form of the configurational force for bodies subject to mechanical loads, heat and multiple diffusing species. The derived second law condition naturally extends the Eshelby energy–momentum tensor to include species diffusion terms. The above second law restriction is then used to derive the condition for the growth of new phases in a body undergoing finite deformation subject to inhomogeneous as well as anisotropic interface stress, and multiple diffusing species. The growth conditions are derived in both current and reference configurations. The statistical temperature-dependent growth velocity is next derived using the Boltzmann distribution. The derived finite deformation form of growth requirement is simplified to obtain the small deformation diffusive void growth condition. Next, a general, finite deformation, arbitrary surface stress form of phase nucleation condition is derived by considering uncertainty in growth of a small nucleus. The probability of nucleation is shown to naturally depend on a theoretical estimate of critical volumetric energy density, which is directly related to the surface stress. The classical nucleation theory is shown to result from a simplified special case of the general criterion. As an application of the developed theory, the classical Blech electromigration experiment is simulated to estimate the critical energy density corresponding to the onset of electromigration voids at Al–TiN interface.

Keywords Interface balance laws · Multispecies diffusion · Inhomogeneous surface stress · Second law conditions · Configurational force · Phase growth condition · Phase nucleation condition · Electromigration void

1 Introduction

Diffusion-driven phase nucleation and growth under mechanical, thermal or electrical fields represents an important class of problems. Void nucleation and growth under the influence of an electrical current (electromigration) is an example of this class of problems. Other examples of such phenomena include crack propagation due to creep [1], dendritic growth in Li-ion batteries [2,3], growth of brittle intermetallic compounds in solder joints [4,5], tissue growth [6] and growth of compounds under chemical vapor deposition [7]. The interplay between stress and diffusion can change the morphology of the phase interface from being

Communicated by Andreas Öchsner.

P. Vaitheeswaran · A. Udupa · S. Sadasiva · G. Subbarayan (✉)
School of Mechanical Engineering, Purdue University, West Lafayette, IN 47907, USA
E-mail: ganeshs@purdue.edu

crack-like to spheroidal [8]. The growth of such heterogeneities can have significant physical as well as physiological effect. For example, growth of cracks at high temperatures due to creep decides the life of pipes, turbines, engines in power plants and aircrafts, and moderating the growth of malignant tissues can aid in recovery of diseased individuals.

The growth of a void is typically attributed to the coalescence of vacancies, which is dependent on the magnitude of the bulk diffusion flux of the vacancies [9]. For instance, computational studies of void growth due to electromigration often rely on the flux of vacancies to predict the growth rate [10,11]. A competing model for void growth is to use the bulk entropy of the system to develop a measure of damage [12]. In these models, a constitutive relation is assumed between the bulk diffusion flux and the various driving forces such as the gradients of chemical potential, hydrostatic stress, temperature or electric potential. This constitutive relation is, however, not derived using established principles of rational mechanics at a phase interface. In other words, the constitutive relation is empirical and does not directly follow from balance laws governing a moving interface. Abeyaratne and Knowles [13] are among the few that use interface balance laws to derive a thermodynamic force driving the evolution of a phase interface. The thermodynamic force, or the configurational force [14,15], determines the energy per unit area of the interface consumed as the phase evolves.

In general, the motion of the interface is influenced by the interfacial stress, which may be anisotropic and inhomogeneous. For instance, electromigration experiments have shown a strong relation between void growth rate and surface energy at the interface [16]. The generalization of the configurational force associated with a moving interface, accounting for arbitrary interfacial stress, appears to be largely missing in the literature. The existing models for interfacial growth, while they assume a constitutive relation between the bulk flux and fields, often do not obey interfacial balance laws or incorporate surface stress in their formulation. Gurtin [15] derives the configurational force for a system with homogeneous, isotropic surface stress. However, to the best of the authors' knowledge, this has not been extended to a general system with anisotropic, inhomogeneous surface stress.

In the context of phase nucleation, transformed fraction models based on the Kolmogorov–Johnson–Mehl–Avrami theory and its extensions [17,18] have been used to estimate the nucleation rate. Although the nucleation process has its roots in statistical mechanics, the classical nucleation criterion is developed using continuum theory [19,20]. Specifically in electromigration, a critical vacancy concentration condition [21,22] is often used to describe the onset of void nucleation [10,23]. Among the other criteria that are used to describe electromigration, Tu et al. proposed that the region of "maximum current crowding" or the region with the highest current density is most susceptible to void nucleation [24,25]. Alternatively, stress-based conditions have also been suggested for nucleation [26–28]. A normal stress condition was used in finite element simulations in [29], while a cohesive zone model was used in [30–32]. Finally, [33,34] have used an entropy-based damage criterion to predict void nucleation in finite element simulations. In general, the above models, similar to the growth criteria, do not follow the principles of rational mechanics to derive the nucleation condition from thermodynamic balance laws and further do not consider the influence of surface stress. Nucleation conditions based on the presence of flaws in free surfaces under homogeneous, isotropic surface stress have been proposed [26,35]. Nevertheless, these models have not been extended to general systems with anisotropic, inhomogeneous surface stress.

In summary, to develop generalized conditions for growth or nucleation of a phase under the influence of mechanical and non-mechanical fields as well as arbitrary surface stress, there is a need to derive the configurational force associated with a moving interface in a body with multiple diffusing species and arbitrary surface stress. This is the first goal of the present paper. The second goal of the paper is to apply the general thermodynamic principles governing the motion of an interface to derive conditions for growth of a phase as well as the nucleation of a new phase. The last goal is to demonstrate the derived theory on a practical problem to deduce a critical material parameter governing the nucleation of electromigration voids.

Specifically, in Sect. 2, we first recapitulate the balance laws in the bulk. Then in Sect. 3, we derive a transport theorem for the interface, motivated by the pioneering work of Truesdell and Toupin [36], which is then used to derive the thermodynamic restrictions at the moving interface. The derived driving force on the phase interface is similar to that in references [14,37], but permits inhomogeneous and anisotropic surface stress. The second law conditions are used to derive a general, finite deformation condition for the growth of a phase in both current and reference configurations in Sect. 4. The mean interface velocity under uncertainty in atomistic phenomena described by the Boltzmann distribution is next derived. We then apply the derived general growth condition by reducing it to the special case of diffusive void growth. Next, in Sect. 5, we derive a general, finite deformation nucleation condition taking into account multiple diffusing species and inhomogeneous surface stress by assuming that statistical uncertainty in the length scale associated with the consumed energy of the moving interface. We show that the classical nucleation theory is a special case of the derived general criterion. The void nucleation probability is shown to naturally depend on a critical value of an energy density, which in turn is shown to depend strongly on the interface surface energy coefficient. The developed ideas are then applied, in Sect. 7 to estimate the critical energy density associated with electromigration in Al–TiN interface.

2 Review of balance laws in the bulk

We follow the procedure described in [14,38] in developing the bulk relations for a multispecies (atoms or molecules) solid. Consider a region Ω of the body $\mathcal{B}$ at an instant in time convecting with the body. $\rho(\mathbf{x}, t)$ is the instantaneous mass density at any point in the region. Since the region Ω convects with the body, $\frac{\mathrm{d}}{\mathrm{d}t}\int_{\Omega}\rho\,\mathrm{d}\Omega = 0$. Let the convecting region contain N species labeled $\alpha = 1, 2, \ldots, N$, and let $\nu^{\alpha}(\mathbf{x}, t)$ denote the instantaneous mass fraction of species α (ratio of species mass density to ρ). The body is assumed to consist entirely of diffusing species such that $\sum_{\alpha}\nu^{\alpha} = 1$, and $\rho^{\alpha} = \rho\nu^{\alpha}$ represents the mass density of species α. Changes in Ω are brought about by the diffusion of species α across the boundary $\partial\Omega$ as well as instantaneous species supply r^{α} measured in mass per unit volume per unit time. The mass flux $\boldsymbol{j}^{\alpha}(\mathbf{x}, t)$ is measured in mass per unit area, per unit time, and assumed positive in the outward normal direction of the surface across which the species is transported. Letting $\mathbf{n}$ denote the outward unit normal to the boundary, the mass balance for the species is,

$$\frac{\mathrm{d}}{\mathrm{d}t}\int_{\Omega}\rho\nu^{\alpha}\,\mathrm{d}\Omega = -\int_{\partial\Omega}\boldsymbol{j}^{\alpha}\cdot\mathbf{n}\,\mathrm{d}\Gamma_{\mathrm{s}} + \int_{\Omega} r^{\alpha}\,\mathrm{d}\Omega \tag{1}$$

which yields, after the application of the divergence theorem as well as the Reynolds transport theorem [38], the following local mass balance for any species α,

$$\rho\dot{\nu}^{\alpha} = -\nabla\cdot\boldsymbol{j}^{\alpha} + r^{\alpha} \tag{2}$$

Since the mass fractions sum to unity at all times, the above expression also implies

$$\sum_{\alpha}\rho\dot{\nu}^{\alpha} = \sum_{\alpha}\left(-\nabla\cdot\boldsymbol{j}^{\alpha} + r^{\alpha}\right) = 0 \tag{3}$$

The tractions acting on the surface of the body cause stress $\boldsymbol{\sigma}$ within the body at any instant. $\boldsymbol{\sigma}\mathbf{n}$ represents the surface traction exerted on Ω across the boundary $\partial\Omega$. The balance of linear and angular momentum requires,

$$\begin{aligned}\frac{\mathrm{d}}{\mathrm{d}t}\int_{\Omega}\rho\mathbf{v}\,\mathrm{d}\Omega &= \int_{\partial\Omega}\boldsymbol{\sigma}\mathbf{n}\,\mathrm{d}\Gamma_{\mathrm{s}} + \int_{\Omega}\rho\mathbf{b}\,\mathrm{d}\Omega\\ \frac{\mathrm{d}}{\mathrm{d}t}\int_{\Omega}\mathbf{x}\times\rho\mathbf{v}\,\mathrm{d}\Omega &= \int_{\partial\Omega}\mathbf{x}\times(\boldsymbol{\sigma}\mathbf{n})\,\mathrm{d}\Gamma_{\mathrm{s}} + \int_{\Omega}\mathbf{x}\times\rho\mathbf{b}\,\mathrm{d}\Omega\end{aligned} \tag{4}$$

where $\mathbf{v}$ is the velocity and $\mathbf{b}$ is the body force per unit mass. These yield the local force and moment balances,

$$\begin{aligned}\rho\mathbf{a} &= \nabla\cdot\boldsymbol{\sigma}^{\mathrm{T}} + \rho\mathbf{b}\\ \boldsymbol{\sigma} &= \boldsymbol{\sigma}^{\mathrm{T}}\end{aligned} \tag{5}$$

with $\mathbf{a}$ being the acceleration.

The accumulation of the specific internal energy e and the kinetic energy within the body is:

$$\begin{aligned}\frac{\mathrm{d}}{\mathrm{d}t}\int_{\Omega}\left(\rho e + \frac{1}{2}\rho\mathbf{v}\cdot\mathbf{v}\right)\mathrm{d}\Omega = &\int_{\partial\Omega}(\boldsymbol{\sigma}\mathbf{n})\cdot\mathbf{v}\,\mathrm{d}\Gamma_{\mathrm{s}} + \int_{\Omega}\rho\mathbf{b}\cdot\mathbf{v}\,\mathrm{d}\Omega\\ &-\int_{\partial\Omega}\boldsymbol{j}^{q}\cdot\mathbf{n}\,\mathrm{d}\Gamma_{\mathrm{s}} + \int_{\Omega}r^{q}\,\mathrm{d}\Omega\\ &-\sum_{\alpha=1}^{N}\left(\int_{\partial\Omega}\mu^{\alpha}\boldsymbol{j}^{\alpha}\cdot\mathbf{n}\,\mathrm{d}\Gamma_{\mathrm{s}} - \int_{\Omega}\mu^{\alpha}r^{\alpha}\,\mathrm{d}\Omega\right)\end{aligned} \tag{6}$$

where $\boldsymbol{j}^q$ is the heat flux assumed positive in the outward normal direction of the surface, r^q is the rate of heat supply, and μ^α is the chemical potential of species α measured in units of energy per unit mass. As before, applying the Reynolds transport theorem, using the divergence theorem on the integral over $\partial\Omega$, and utilizing the mass balance relation Eq. (3), one obtains the local rate of change of internal energy as

$$\rho\dot{e} = \boldsymbol{\sigma} : \mathbf{D} - \nabla \cdot \boldsymbol{j}^q + r^q - \sum_{\alpha=1}^{N} \left(\boldsymbol{j}^\alpha \cdot \nabla\mu^\alpha - \rho\mu^\alpha\dot{\nu}^\alpha\right) \tag{7}$$

where $\mathbf{D}$ is the symmetric part of the velocity gradient tensor $\nabla\mathbf{v}^{\mathrm{T}}$. The local form of entropy imbalance is defined as:

$$\rho\dot{\eta} \geq -\nabla \cdot \left(\frac{\boldsymbol{j}^q}{T}\right) + \frac{r^q}{T} \tag{8}$$

where η is the specific internal entropy and T is the absolute temperature. Defining the free energy as $\psi = e - \eta T$, using the local form of entropy imbalance Eq. (8), finally the local form of the free energy imbalance is obtained as:

$$\rho(\dot{\psi} + \eta\dot{T}) \leq \boldsymbol{\sigma} : \mathbf{D} - \frac{1}{T}\boldsymbol{j}^q \cdot \nabla T - \sum_{\alpha=1}^{N} \left(\boldsymbol{j}^\alpha \cdot \nabla\mu^\alpha - \rho\mu^\alpha\dot{\nu}^\alpha\right) \tag{9}$$

Thus, all thermodynamically permissible processes in the bulk must are consistent with Eq. (9). The free energy ψ is a function of the deformation, the species concentration, and the temperature $\psi \equiv \psi\,(\mathbf{F}, \nu^\alpha, T)$, where $\mathbf{F}$ is the deformation gradient. Using the chain rule to compute $\dot{\psi}$ and writing $\boldsymbol{\sigma} : \mathbf{D} = \boldsymbol{\sigma} : \nabla\mathbf{v}^{\mathrm{T}} = \boldsymbol{\sigma} : \dot{\mathbf{F}}\mathbf{F}^{-1}$ gives,

$$\begin{aligned}&\left(\rho\frac{\partial\psi}{\partial\mathbf{F}} - \boldsymbol{\sigma}\mathbf{F}^{-\mathrm{T}}\right) : \dot{\mathbf{F}} + \sum_{\alpha=1}^{N}\left(\frac{\partial\psi}{\partial\nu^\alpha} - \mu^\alpha\right)\rho\dot{\nu^\alpha} + \left(\frac{\partial\psi}{\partial T} + \eta\right)\rho\dot{T}\\ &+ \sum_{\alpha=1}^{N}\boldsymbol{j}^\alpha \cdot \nabla\mu^\alpha + \frac{1}{T}\boldsymbol{j}^q \cdot \nabla T \leq 0\end{aligned} \tag{10}$$

Since this inequality has to hold for arbitrary values of $\dot{\mathbf{F}}$, $\dot{\nu^\alpha}$ and $\dot{T}$ we get the constitutive equations,

$$\boldsymbol{\sigma} = \rho\frac{\partial\psi}{\partial\mathbf{F}}\mathbf{F}^{\mathrm{T}} \tag{11}$$

$$\mu^\alpha = \frac{\partial\psi}{\partial\nu^\alpha} \quad \forall\alpha \tag{12}$$

$$\eta = -\frac{\partial\psi}{\partial T} \tag{13}$$

The terms within the parentheses hence vanish. Finally, since temperature is always positive, the free energy inequality is satisfied by constitutive relations of form,

$$\boldsymbol{j}^\alpha = -\mathbf{M}^\alpha\nabla\mu^\alpha \quad \forall\alpha \tag{14}$$

$$\boldsymbol{j}^q = -\mathbf{k}\nabla T \tag{15}$$

where $\mathbf{M}^\alpha$ is a positive definite mobility tensor for species α and $\mathbf{k}$ is a positive definite thermal conductivity tensor. Equation (14) describes Fick's first law of diffusion for each species α, while Eq. (15) is the Fourier law of heat conduction.

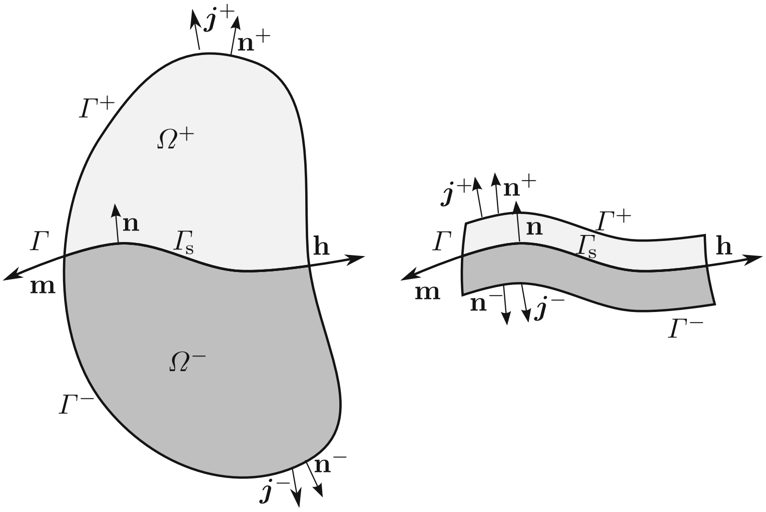

Fig. 1 Control volume (interface "pillbox") with generalized field and fluxes

3 Derivation of balance laws at the interface

The development in this section is motivated by the pioneering work of Truesdell and Toupin [36]. The approach followed is to make a systematic analogy to the bulk balance laws described in Sect. 2, including in the explicit use of an entropic inequality condition on the interface. Additionally, analogous to bulk derivation, surface quantities corresponding to mass, momentum, internal energy, entropy and free energy are introduced as variables and resolved through the derived thermodynamic restrictions. The resulting form of the driving force on the phase interface is similar to that derived in [14,37], but the derivation here allows inhomogeneous and anisotropic surface stress.

3.1 Interface transport theorem

Prior to deriving the balance laws at the interface, we first derive the interface transport theorem for a scalar field on the interface that then serves to provide the basis for derivation of mass, momentum and energy balances at the interface. The interface is modeled to convect with the body in the present work. To connect the bulk fields with the interface, an interface "pillbox" (Fig. 1) is typically used to derive local balance relations at interfaces.

Consider the domain $\Omega = \Omega^- \cup \Omega^+$ divided by the interface Γ shown in Fig. 1 with the subregion Γ_s within the control volume. Ω^- and Ω^+ are bounded otherwise by Γ^- and Γ^+. An arbitrary field $\phi(\mathbf{x}, t)$ is considered, with the values in each of the phases specified by $\phi^-(\mathbf{x}, t)$ and $\phi^+(\mathbf{x}, t)$. The balance law for the domain of each phase can now be written as,

$$\frac{\mathrm{d}}{\mathrm{d}t}\left(\int_{\Omega^i} \phi^i \,\mathrm{d}\Omega\right) = -\int_{\Gamma^i} \boldsymbol{j}^i \cdot \mathbf{n}^i \,\mathrm{d}\Gamma_s - \int_{\Gamma_s} \boldsymbol{j}^i \cdot \mathbf{n}^i \,\mathrm{d}\Gamma_s + \int_{\Omega^i} r^i \,\mathrm{d}\Omega \qquad i = -, + \tag{16}$$

where $\boldsymbol{j}$ refers to the flux of the field ϕ, while r denotes volumetric generation. The interface is now considered as a separate domain, bounded by the curve $\partial\Gamma_s$ (Fig. 1). The superficial field on the interface ϕ_s is changed by inflows due to a flux $\boldsymbol{h}$ on the boundary $\partial\Gamma_s$ of the interface, the flux exchanges $\boldsymbol{j}^i$ with the bulk domains on either side, and the spontaneous generation rate r_s. The normal to the curve $\partial\Gamma_s$ in the tangent plane of Γ is denoted $\mathbf{m}$ (see Fig. 2). The balance law for the interface is now written as,

$$\frac{\mathrm{d}}{\mathrm{d}t}\int_{\Gamma_s} \phi_s \,\mathrm{d}\Gamma_s = -\oint_{\partial\Gamma_s} \boldsymbol{h}.\mathbf{m} \,\mathrm{d}c + \sum_{i=-,+} \int_{\Gamma_s} \boldsymbol{j}^i \cdot \mathbf{n}^i \,\mathrm{d}\Gamma_s + \int_{\Gamma_s} r_s \,\mathrm{d}\Gamma_s \tag{17}$$

To be able to define a transport theorem for the interface pillbox, Eqs. (16) and (17) need to be combined together. Utilizing the expressions for the material derivatives on the left-hand sides of Eqs. (16) and (17)

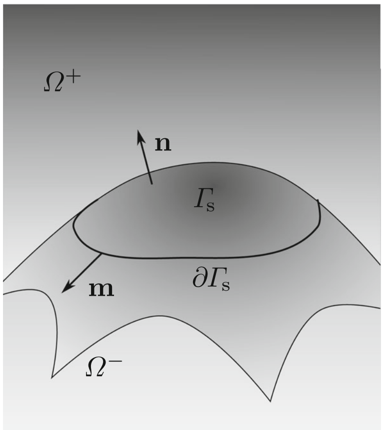

Fig. 2 Schematic showing the definition of the normals to the interface and to the boundary of the interface subregion Γ_s

(derived in Appendices B, and C on the basis of surface identities given in Appendix A), following [36], the combined bulk and surface balances yield,

$$\begin{aligned}\sum_{i=-,+}&\left(\int_{\Omega^i}\frac{\partial\phi^i}{\partial t}\,\mathrm{d}\Omega+\int_{\Gamma^i}\phi^i v_n^i\,\mathrm{d}\Gamma_\mathrm{s}+\int_{\Gamma_\mathrm{s}}\phi^i v_{\mathrm{s_n}}^i\,\mathrm{d}\Gamma_\mathrm{s}\right)\\&+\int_{\Gamma_\mathrm{s}}\left(\dot{\phi}_\mathrm{s}+\phi_\mathrm{s}\nabla_\mathrm{s}\cdot\mathbf{v}_\mathrm{s}\right)\mathrm{d}\Gamma_\mathrm{s}\\&=\sum_{i=-,+}\left(-\int_{\Gamma^i}\boldsymbol{j}^i\cdot\mathbf{n}^i\,\mathrm{d}\Gamma_\mathrm{s}+\int_{\Omega^i}r^i\,\mathrm{d}\Omega\right)-\oint_{\partial\Gamma_\mathrm{s}}\boldsymbol{h}.\mathbf{m}\,\mathrm{d}c+\int_{\Gamma_\mathrm{s}}r_\mathrm{s}\,\mathrm{d}\Gamma_\mathrm{s}\end{aligned}\tag{18}$$

where $v_n^i=\mathbf{v}^i\cdot\mathbf{n}^i$, $v_{\mathrm{s_n}}^i=\mathbf{v}_\mathrm{s}^i\cdot\mathbf{n}^i$. The following simplifications are made to Eq. (18).

1. The outer control surfaces Γ^-, Γ^+ are infinitesimally close to the inner control surface Γ_s. As $\Gamma^-, \Gamma^+\to\Gamma_\mathrm{s}$, $\Omega\to 0$ and the bulk integral terms drop out.
2. $\mathbf{n}^-$ is set equal to $\mathbf{n}$ on Γ_s. This implies that $\mathbf{n}^+=-\mathbf{n}$ on Γ_s. Thus, as $\Omega\to 0$, $\mathbf{n}^-=-\mathbf{n}$ on Γ^-, and $\mathbf{n}^+=\mathbf{n}$ on Γ^+.

These simplifications along with the use of the surface divergence theorem of Eq. (96) reduce Eq. (18) to,

$$\begin{aligned}&\int_{\Gamma_\mathrm{s}}\left(-\left[\!\left[\phi\left(v_{\mathrm{s_n}}-v_n\right)\right]\!\right]+\dot{\phi}_\mathrm{s}+\phi_\mathrm{s}\nabla_\mathrm{s}\cdot\mathbf{v}_\mathrm{s}\right)\mathrm{d}\Gamma_\mathrm{s}\\&\quad=\int_{\Gamma_\mathrm{s}}\left(-\left[\!\left[\boldsymbol{j}^\phi\right]\!\right]\cdot\mathbf{n}-\nabla_\mathrm{s}\cdot\boldsymbol{h}_\mathbf{t}^\phi+r_\mathrm{s}^\phi\right)\mathrm{d}\Gamma_\mathrm{s}\end{aligned}\tag{19}$$

where the jump terms are defined as $[\![\cdot]\!]=\left(\cdot^+-\cdot^-\right)$ and $\left(v_{\mathrm{s_n}}-v_n\right)=\left(\mathbf{v}_\mathrm{s}-\mathbf{v}\right)\cdot\mathbf{n}$; $\boldsymbol{h}_\mathbf{t}^\phi=\mathbf{P}\boldsymbol{h}^\phi$ is the tangential component of the flux $\boldsymbol{h}^\phi$ with $\mathbf{P}$ being the surface projection tensor defined in Eq. (88). The superscript ϕ serves to remind the quantity whose flux is on the right-hand side. Since Eq. (19) must be valid on every arbitrary subregion Γ_s of Γ, we arrive at the local form of the interface transport theorem:

$$-\left[\!\left[\phi\left(v_{\mathrm{s_n}}-v_n\right)\right]\!\right]+\dot{\phi}_\mathrm{s}+\phi_\mathrm{s}\nabla_\mathrm{s}\cdot\mathbf{v}_\mathrm{s}=-\left[\!\left[\boldsymbol{j}^\phi\right]\!\right]\cdot\mathbf{n}-\nabla_\mathrm{s}\cdot\boldsymbol{h}_\mathbf{t}^\phi+r_\mathrm{s}^\phi\quad\text{on }\Gamma\tag{20}$$

where the left-hand side of the above expression represents the accumulation of bulk and interface fields due to bulk normal fluxes and the interface flux.

3.2 Balance laws at the interface

The general interface transport theorem of Eq. (20) can be applied to various conserved quantities such as species mass, momentum and energy, by replacing ϕ with the appropriate conserved quantity to obtain the balance law. The species mass balance at the interface is obtained by replacing the bulk field ϕ by $\rho\nu^\alpha$, the mass flux $\boldsymbol{j}^\phi$ of the diffusing species α by $\boldsymbol{j}^\alpha$, and the tangential interface flux $\boldsymbol{h}_\mathbf{t}^\phi$ by the surface mass flux $\boldsymbol{h}_\mathbf{t}^\alpha$. Also, the interface is considered massless, and therefore, surface mass excess, ϕ_s, is ignored. The rate of spontaneous generation of species α at the surface (as due to a chemical reaction) is denoted r_s^α. Substituting in Eq. (20), we obtain the species balance as,

$$-\left[\!\left[\rho\nu^\alpha\left(v_{\mathrm{s_n}}-v_n\right)\right]\!\right] = -[\![\boldsymbol{j}^\alpha]\!]\cdot\mathbf{n} - \nabla_\mathrm{s}\cdot\boldsymbol{h}_\mathbf{t}^\alpha + r_\mathrm{s}^\alpha \tag{21}$$

The momentum balance at the interface is obtained by considering momentum in an arbitrary, but fixed direction $\hat{\mathbf{n}}$. By analogy to the bulk relation Eq. (4), we choose the field ϕ to be the momentum in the direction $\hat{\mathbf{n}}$, that is, $\phi = \rho\mathbf{v}\cdot\hat{\mathbf{n}}$. Since the negative of the normal component of the bulk flux enters the domain, by analogy of Eq. (4), $-\boldsymbol{j}^i\cdot\mathbf{n}^i = \hat{\mathbf{n}}\cdot\boldsymbol{\sigma}\mathbf{n}^i$, and the flux is defined as $\boldsymbol{j}^\mathbf{v} = -\boldsymbol{\sigma}\hat{\mathbf{n}}$ so that the normal component of this quantity defines the traction component in the direction $\hat{\mathbf{n}}$. Similarly, since the component of the surface flux normal to the boundary $\partial\Gamma_\mathrm{s}$ enters the surface, the surface flux is defined as $\boldsymbol{h}^\mathbf{v} = -\boldsymbol{\sigma}_\mathrm{s}\hat{\mathbf{n}}$ with a symmetric surface stress $\boldsymbol{\sigma}_\mathrm{s}$ such that traction component $\boldsymbol{h}^\mathbf{v}\cdot\mathbf{m}$ acts on the boundary $\partial\Gamma_\mathrm{s}$ tangent to the plane of the interface. Now, assuming that the interface is massless, and that the spontaneous generation of momentum is negligible, i.e., ϕ_s and r_s are zero, substituting in Eq. (20), we obtain the momentum balance as:

$$-\left[\!\left[\rho\mathbf{v}\left(v_{\mathrm{s_n}}-v_n\right)\right]\!\right]\cdot\hat{\mathbf{n}} = [\![\boldsymbol{\sigma}\hat{\mathbf{n}}]\!]\cdot\mathbf{n} - \nabla_\mathrm{s}\cdot\boldsymbol{h}_\mathbf{t}^\mathbf{v} \tag{22}$$

Furthermore, $\boldsymbol{h}_\mathbf{t}^\mathbf{v} = \mathbf{P}\boldsymbol{h}^\mathbf{v} = -\mathbf{P}\boldsymbol{\sigma}_\mathrm{s}\hat{\mathbf{n}}$. Since $\hat{\mathbf{n}}$ is arbitrary, constant and nonzero, Eq. (22) yields:

$$-\left[\!\left[\rho\mathbf{v}\left(v_{\mathrm{s_n}}-v_n\right)\right]\!\right] = [\![\boldsymbol{\sigma}]\!]\,\mathbf{n} + \nabla_\mathrm{s}\cdot(\mathbf{P}\boldsymbol{\sigma}_\mathrm{s}) \tag{23}$$

If the surface stress is homogeneous and isotropic, i.e., $\boldsymbol{\sigma}_\mathrm{s} = \gamma\mathbf{I}$, bulk inertial effects are small, then the momentum jump can be ignored, and using Eq. (93), we can obtain the Laplace–Young equation:

$$-\mathbf{n}\cdot[\![\boldsymbol{\sigma}]\!]\,\mathbf{n} = \gamma\kappa \tag{24}$$

where κ is the total curvature of the interface.

As with momentum balance, the interface energy balance is obtained by analogy of Eq. (6). Thus, the bulk field is $\phi = \rho e + \frac{1}{2}\rho\mathbf{v}\cdot\mathbf{v}$ and bulk energy flux is $\boldsymbol{j}^e = -\boldsymbol{\sigma}\mathbf{v} + \boldsymbol{j}^q + \sum_{\alpha=1}^N \mu^\alpha\boldsymbol{j}^\alpha$. The surface field ϕ_s is given by the internal energy per unit area, e_s. By analogy to interface momentum balance, the tangential component of the surface flux corresponding to internal energy accumulation is given by $\boldsymbol{h}_\mathbf{t}^e = -\mathbf{P}\boldsymbol{\sigma}_\mathrm{s}\mathbf{v}_\mathrm{s} + \boldsymbol{h}^q + \sum_{\alpha=1}^N \mu_\mathrm{s}^\alpha\boldsymbol{h}_\mathbf{t}^\alpha$. Thus, the interface energy balance relation is:

$$\begin{aligned}
&-\left[\!\left[\phi\left(v_{\mathrm{s_n}}-v_n\right)\right]\!\right] + \dot{\phi}_\mathrm{s} + \phi_\mathrm{s}\nabla_\mathrm{s}\cdot\mathbf{v}_\mathrm{s} \\
&\quad= -\left[\!\left[-\boldsymbol{\sigma}\mathbf{v} + \boldsymbol{j}^q + \sum_{\alpha=1}^N \mu^\alpha\boldsymbol{j}^\alpha\right]\!\right]\cdot\mathbf{n} - \nabla_\mathrm{s}\cdot\left(-\mathbf{P}\boldsymbol{\sigma}_\mathrm{s}\mathbf{v}_\mathrm{s} + \boldsymbol{h}^q + \sum_{\alpha=1}^N \mu_\mathrm{s}^\alpha\boldsymbol{h}_\mathbf{t}^\alpha\right) \\
&\qquad + r_\mathrm{s}^q + \sum_{\alpha=1}^N \mu_\mathrm{s}^\alpha r_\mathrm{s}^\alpha
\end{aligned} \tag{25}$$

Using the interface species mass balance Eq. (21) and utilizing the surface identities in Appendix A, the above equation simplifies to:

$$\begin{aligned}
&-\left[\!\left[\left(\rho e + \frac{1}{2}\rho\mathbf{v}\cdot\mathbf{v}\right)\left(v_{\mathrm{s_n}}-v_n\right)\right]\!\right] + \dot{e}_\mathrm{s} + e_\mathrm{s}\nabla_\mathrm{s}\cdot\mathbf{v}_\mathrm{s} \\
&\quad= [\![\boldsymbol{\sigma}\mathbf{v}]\!]\cdot\mathbf{n} - [\![\boldsymbol{j}^q]\!]\cdot\mathbf{n} - \nabla_\mathrm{s}\cdot\boldsymbol{h}_\mathbf{t}^q + r_\mathrm{s}^q \\
&\qquad - \sum_{\alpha=1}^N\left(\mu_\mathrm{s}^\alpha\left[\!\left[\rho\nu^\alpha\left(v_{\mathrm{s_n}}-v_n\right)\right]\!\right] + \boldsymbol{h}_\mathbf{t}^\alpha\cdot\nabla_\mathrm{s}\,\mu_\mathrm{s}^\alpha\right) \\
&\qquad + \sum_{\alpha=1}^N\left(-[\![\mu^\alpha\boldsymbol{j}^\alpha]\!] + \mu_\mathrm{s}^\alpha[\![\boldsymbol{j}^\alpha]\!]\right)\cdot\mathbf{n} \\
&\qquad + \nabla_\mathrm{s}\cdot(\mathbf{P}\boldsymbol{\sigma}_\mathrm{s}\mathbf{v}_\mathrm{s})
\end{aligned} \tag{26}$$

The interface entropy inequality can be obtained analogous to the bulk entropy inequality Eq. (8). Let η denote the bulk specific internal entropy and η_s denote the entropy per unit area of the interface. The external sources of entropy are the bulk heat flux $\boldsymbol{j}^q$, surface heat flux $\boldsymbol{h}^q$ and the surface heat generation r^q_s. Following the pillbox procedure in Sect. 3.1 gives the interface entropy imbalance inequality,

$$-\left[\!\left[\rho\eta\left(v_{\mathrm{s}_\mathrm{n}}-v_n\right)\right]\!\right]+\dot{\eta}_\mathrm{s}+\eta_\mathrm{s}\nabla_\mathrm{s}\cdot\mathbf{v}_\mathrm{s}\geq-\left[\!\left[\frac{\boldsymbol{j}^q}{T}\right]\!\right]\cdot\mathbf{n}-\nabla_\mathrm{s}\cdot\frac{\boldsymbol{h}^q_\mathbf{t}}{T_\mathrm{s}}+\frac{r^q_\mathrm{s}}{T_\mathrm{s}} \tag{27}$$

where T_s is the surface temperature.

Defining the specific free energy, $\psi=e-\eta T$ and its interface equivalent, the free energy per unit area of the interface, $\psi_\mathrm{s}=e_\mathrm{s}-\eta_\mathrm{s}T_\mathrm{s}$, the free energy inequality is obtained by using the first and second laws of thermodynamics [Eqs. (26) and (27)], assuming continuity of chemical potential across the interface, i.e.,

$$[\![\mu^\alpha]\!]=0,\quad \mu^\alpha_\mathrm{s}=\mu^\alpha \tag{28}$$

and under the assumption of continuity of temperature, i.e.,

$$[\![T]\!]=0,\quad T_\mathrm{s}=T \tag{29}$$

we get:

$$\begin{aligned}
&-\left[\!\!\left[\left(\rho\psi+\frac{1}{2}\rho\mathbf{v}\cdot\mathbf{v}\right)\left(v_{\mathrm{s}_\mathrm{n}}-v_n\right)\right]\!\!\right]+\dot{\psi}_\mathrm{s}+\eta_\mathrm{s}\dot{T}_\mathrm{s}\\
&\quad+\psi_\mathrm{s}\nabla_\mathrm{s}\cdot\mathbf{v}_\mathrm{s}+\frac{1}{T_\mathrm{s}}\boldsymbol{h}^q_\mathbf{t}\cdot\nabla_\mathrm{s}T_\mathrm{s}\\
&\quad\leq-\left[\!\left[\rho\mathbf{v}_\mathrm{s}\cdot\mathbf{v}\left(v_{\mathrm{s}_\mathrm{n}}-v_n\right)\right]\!\right]-[\![\boldsymbol{\sigma}\left(\mathbf{v}_\mathrm{s}-\mathbf{v}\right)]\!]\cdot\mathbf{n}-\left[\nabla_\mathrm{s}\cdot(\mathbf{P}\boldsymbol{\sigma}_\mathrm{s})\right]\cdot\mathbf{v}_\mathrm{s}\\
&\quad-\sum_{\alpha=1}^{N}\left(\left[\!\left[\rho\mu^\alpha\nu^\alpha\left(v_{\mathrm{s}_\mathrm{n}}-v_n\right)\right]\!\right]+\boldsymbol{h}^\alpha_\mathbf{t}\cdot\nabla_\mathrm{s}\mu^\alpha_\mathrm{s}\right)\\
&\quad+\nabla_\mathrm{s}\cdot(\mathbf{P}\boldsymbol{\sigma}_\mathrm{s}\mathbf{v}_\mathrm{s})
\end{aligned} \tag{30}$$

where we have substituted for $[\![\boldsymbol{\sigma}\mathbf{v}]\!]\cdot\mathbf{n}$ from the expression derived in Eq. (121) of Appendix E. The right-hand side indicates the work that is being done on the control volume due to surface tractions and diffusion. The free energy increase in the system is given to be less than or equal to the right-hand side by the second law. Substituting $\nabla_\mathrm{s}\cdot(\mathbf{P}\boldsymbol{\sigma}_\mathrm{s}\mathbf{v}_\mathrm{s})=[\nabla_\mathrm{s}\cdot(\mathbf{P}\boldsymbol{\sigma}_\mathrm{s})]\cdot\mathbf{v}_\mathrm{s}+\mathbf{P}\boldsymbol{\sigma}_\mathrm{s}:\nabla_\mathrm{s}\mathbf{v}_\mathrm{s}$, and keeping in mind that $\boldsymbol{\sigma}_\mathrm{s}$ and $\mathbf{P}$ are symmetric, we get,

$$\begin{aligned}
&-\left[\!\left[\rho\left(\frac{\mathbf{v}}{2}-\mathbf{v}_\mathrm{s}\right)\cdot\mathbf{v}\left(v_{\mathrm{s}_\mathrm{n}}-v_n\right)\right]\!\right]+\dot{\psi}_\mathrm{s}+\eta_\mathrm{s}\dot{T}_\mathrm{s}\\
&\quad+\psi_\mathrm{s}\nabla_\mathrm{s}\cdot\mathbf{v}_\mathrm{s}-\boldsymbol{\sigma}_\mathrm{s}\mathbf{P}:(\nabla_\mathrm{s}\mathbf{v}_\mathrm{s})^\mathrm{T}\\
&\quad-\left[\!\!\left[(\mathbf{v}_\mathrm{s}-\mathbf{v})\cdot\left(\rho\psi\mathbf{I}-\boldsymbol{\sigma}-\rho\sum_{\alpha=1}^{N}\mu^\alpha\nu^\alpha\mathbf{I}\right)\mathbf{n}\right]\!\!\right]\\
&\quad+\sum_{\alpha=1}^{N}\boldsymbol{h}^\alpha_\mathbf{t}\cdot\nabla_\mathrm{s}\mu^\alpha_\mathrm{s}+\frac{1}{T_\mathrm{s}}\boldsymbol{h}^q_\mathbf{t}\cdot\nabla_\mathrm{s}T_\mathrm{s}\leq 0
\end{aligned} \tag{31}$$

Finally, we postulate that the surface free energy is a function of temperature and a scalar state variable ξ_s. That is, $\psi_\mathrm{s}\equiv\psi_\mathrm{s}(\xi_\mathrm{s},T_\mathrm{s})$. Thus, we can write,

$$\dot{\psi}_\mathrm{s}(\xi_\mathrm{s},T_\mathrm{s})=\frac{\partial\psi_\mathrm{s}}{\partial\xi_\mathrm{s}}\dot{\xi}_\mathrm{s}+\frac{\partial\psi_\mathrm{s}}{\partial T_\mathrm{s}}\dot{T}_\mathrm{s} \tag{32}$$

Ignoring inertial effects or the higher-order velocity terms, utilizing the derivations for $(\nabla_\mathrm{s}\,\mathbf{v}_\mathrm{s})^\mathrm{T}$ and $\nabla_\mathrm{s}\cdot\mathbf{v}_\mathrm{s}$ given in Appendix D, Eqs. (116) and (118), we can now rewrite Eq. (31) as

$$\begin{aligned}&\frac{\partial\psi_\mathrm{s}}{\partial\xi_\mathrm{s}}\dot{\xi}_\mathrm{s}+\left(\frac{\partial\psi_\mathrm{s}}{\partial T_\mathrm{s}}+\eta_\mathrm{s}\right)\dot{T}_\mathrm{s}\\&+(\psi_\mathrm{s}\mathbf{I}-\boldsymbol{\sigma}_\mathrm{s})\,\mathbf{P}:\overset{\triangle}{\mathbf{F}}\mathbf{G}\\&-\left[\!\!\left[(\mathbf{v}_\mathrm{s}-\mathbf{v})\cdot\left(\rho\psi\mathbf{I}-\boldsymbol{\sigma}-\rho\sum_{\alpha=1}^{N}\mu^\alpha\nu^\alpha\mathbf{I}\right)\mathbf{n}\right]\!\!\right]\\&+\sum_{\alpha=1}^{N}\boldsymbol{h}_\mathbf{t}^\alpha\cdot\nabla_\mathrm{s}\,\mu_\mathrm{s}^\alpha+\frac{1}{T_\mathrm{s}}\boldsymbol{h}_\mathbf{t}^q\cdot\nabla_\mathrm{s}\,T_\mathrm{s}\le 0\end{aligned}\tag{33}$$

where $\overset{\triangle}{\mathbf{F}}$ is the convected time derivative of the deformation gradient defined in Eq. (117).

Since Eq. (33) has to be satisfied for arbitrary values of the rates $\dot{\xi}_\mathrm{s}$, $\overset{\triangle}{\mathbf{F}}$, $\dot{T}_\mathrm{s}$, the following conditions, which are analogous to bulk definitions of Eqs. (11) and (13), have to hold:

$$\frac{\partial\psi_\mathrm{s}}{\partial\xi_\mathrm{s}}=0\tag{34}$$

$$(\psi_\mathrm{s}\mathbf{I}-\boldsymbol{\sigma}_\mathrm{s})\,\mathbf{P}=0\tag{35}$$

$$\eta_\mathrm{s}=-\frac{\partial\psi_\mathrm{s}}{\partial T_\mathrm{s}}\tag{36}$$

Furthermore, to satisfy Eq. (33), the following inequalities also have to hold on the interface,

$$-\left[\!\!\left[(\mathbf{v}_\mathrm{s}-\mathbf{v})\cdot\left(\rho\psi\mathbf{I}-\boldsymbol{\sigma}-\rho\sum_{\alpha=1}^{N}\mu^\alpha\nu^\alpha\mathbf{I}\right)\mathbf{n}\right]\!\!\right]\le 0\tag{37}$$

$$\boldsymbol{h}_\mathbf{t}^\alpha\cdot\nabla_\mathrm{s}\,\mu_\mathrm{s}^\alpha\le 0\quad\forall\alpha\tag{38}$$

$$\boldsymbol{h}_\mathbf{t}^q\cdot\nabla_\mathrm{s}\,T_\mathrm{s}\le 0\tag{39}$$

Equation (35) implies that the rows of $(\psi_\mathrm{s}\mathbf{I}-\boldsymbol{\sigma}_\mathrm{s})$ are in the surface normal direction $\mathbf{n}$. This in turn implies that the quantity has unit rank with a single out-of-plane eigenvector. Thus, for arbitrary surface normal $\mathbf{n}$ and hence arbitrary $\mathbf{P}$, for condition Eq. (35) to hold

$$\det(\psi_\mathrm{s}\mathbf{I}-\boldsymbol{\sigma}_\mathrm{s})=0\tag{40}$$

This condition is trivially achieved if the surface stress is homogeneous and isotropic, i.e., if $\boldsymbol{\sigma}_\mathrm{s}=\gamma\mathbf{I}$. The conditions in Eqs. (38) and (39) are satisfied by constitutive relations of the following form:

$$\boldsymbol{h}_\mathbf{t}^\alpha=-\mathbf{M}_\mathrm{s}^\alpha\nabla_\mathrm{s}\,\mu_\mathrm{s}^\alpha\tag{41}$$

$$\boldsymbol{h}_\mathbf{t}^q=-\mathbf{k}_\mathrm{s}\nabla_\mathrm{s}\,T_\mathrm{s}\tag{42}$$

where $\mathbf{M}_\mathrm{s}^\alpha$ is a positive definite surface mobility tensor for the species α and $\mathbf{k}_\mathrm{s}$ is a positive definite heat conductivity tensor on the surface. The above equations are the surface analogs of the bulk versions of Fick's law and Fourier's law [Eqs. (14), (15)].

As derived in Appendix F, in the absence of inertial forces, Eq. (37) can be restated in the reference configuration using Eq. (127),

$$\mathbf{V}_\mathrm{S}\cdot[\![\Sigma_\nu-\boldsymbol{\sigma}_\mathrm{I}]\!]\,\mathbf{N}\ge 0\quad\text{on }\Gamma_{\mathrm{s}_0}\tag{43}$$

where

$$\Sigma_\nu=\Sigma_0-\rho_0\sum_{\alpha=1}^{N}\mu_0^\alpha\nu_0^\alpha\mathbf{I}\tag{44}$$

is an extension to the Eshelby energy–momentum tensor [39] $\Sigma_0 = (\rho_0\psi_0\mathbf{I} - \nabla_0\mathbf{U}\boldsymbol{\sigma}_{\mathrm{I}})$, with $\boldsymbol{\sigma}_{\mathrm{I}}$ being the first Piola–Kirchhoff stress tensor; $\mathbf{U}$ is the displacement in reference coordinates and $\Gamma_{\mathrm{s}0}$ is the subsurface viewed in the reference configuration. Eshelby also suggests $\Sigma_0^* = \Sigma_0 - \boldsymbol{\sigma}_{\mathrm{I}}$ as an energy–momentum tensor with greater utility for estimating the force on a defect [39].

The jump $[\![\Sigma_\nu - \boldsymbol{\sigma}_{\mathrm{I}}]\!]$ represents a conserved quantity that will integrate to zero within a homogeneous domain. In this sense, it is an extension to the path-independent J-integral of fracture mechanics [40] to bodies with multiple diffusing species. The conjugate to the reference interface velocity $\mathbf{V}_{\mathrm{s}}$, namely $[\![\Sigma_\nu - \boldsymbol{\sigma}_{\mathrm{I}}]\!]\,\mathbf{N}$, is the reference configurational force associated with the motion of the interface.

4 Conditions for phase growth

During the growth of the phases, Eq. (37) should be satisfied at each point on Γ and at all instants of time. It is convenient, however, to derive the growth criterion in the reference configuration using Eq. (43), specifically the alternative form of the equation as listed in Eq. (126). We begin by decomposing the surface velocity into tangential and normal components in the reference configuration $\mathbf{V}_{\mathrm{S}} = \mathbf{V}_{\mathrm{S_T}} + V_{\mathrm{S_N}}\mathbf{N}$, where $\mathbf{N}$ is the surface normal vector with the convention that $\mathbf{N}$ points from Phase $-$ into Phase $+$ (see Fig. 1). Thus, the left-hand side of Eq. (43) can be written as

$$\left(\mathbf{V}_{\mathrm{S_T}} + V_{\mathrm{S_N}}\mathbf{N}\right)\cdot[\![\Sigma_\nu - \boldsymbol{\sigma}_{\mathrm{I}}]\!]\,\mathbf{N} = \mathbf{V}_{\mathrm{S_T}}\cdot\left[\!\!\left[\rho_0\left(\psi_0 - \sum_{\alpha=1}^{N}\mu_0^\alpha\nu_0^\alpha\right)\mathbf{I} - \mathbf{F}^{\mathrm{T}}\boldsymbol{\sigma}_{\mathrm{I}}\right]\!\!\right]\mathbf{N} + V_{\mathrm{S_N}}\mathbf{N}\cdot[\![\Sigma_\nu - \boldsymbol{\sigma}_{\mathrm{I}}]\!]\,\mathbf{N} \tag{45}$$

where $\mathbf{F}$ is the deformation gradient with the inverse $\mathbf{F}^{-1} = \mathbf{G}$. Simplifying, the second law condition of Eq. (45) reduces to requiring:

$$-\,[\![\mathbf{F}\mathbf{V}_{\mathrm{S_T}}\cdot\boldsymbol{\sigma}_{\mathrm{I}}\mathbf{N}]\!] + V_{\mathrm{S_N}}\mathbf{N}\cdot[\![\Sigma_\nu - \boldsymbol{\sigma}_{\mathrm{I}}]\!]\,\mathbf{N} \geq 0 \quad \text{on } \Gamma_{\mathrm{s}0} \tag{46}$$

In the above expression, it was possible to move $\mathbf{V}_{\mathrm{S_T}}$ and $\mathbf{N}$ inside the jump term since for a coherent interface (see Appendix D), $[\![\mathbf{N}]\!] = [\![\mathbf{V}_{\mathrm{S}}]\!] = 0$ and hence $[\![V_{\mathrm{S_N}}\mathbf{N}]\!] = 0$ leading to $[\![\mathbf{V}_{\mathrm{S}}]\!] = [\![V_{\mathrm{S_N}}\mathbf{N} + \mathbf{V}_{\mathrm{S_T}}]\!] = [\![\mathbf{V}_{\mathrm{S_T}}]\!] = 0$.

The relation between the normal in the reference configuration and in the current configuration is obtained using the differential surface relation Eq. (123):

$$\mathbf{N} = \frac{J_{\mathrm{s}}}{J^i}\mathbf{F}^{i\,\mathrm{T}}\mathbf{n} \tag{47}$$

where i represents either $+$ or $-$ Phase and,

$$J_{\mathrm{s}} = \frac{\mathrm{d}\Gamma_{\mathrm{s}}}{\mathrm{d}\Gamma_{\mathrm{s}0}} = \frac{J^i}{\sqrt{\mathbf{n}\cdot\mathbf{F}^i\mathbf{F}^{i\,\mathrm{T}}\mathbf{n}}} \tag{48}$$

We note that $J_{\mathrm{s}} > 0$, $[\![J_{\mathrm{s}}]\!] = 0$ due to coherence of the interface. Also, $\mathbf{F}\mathbf{V}_{\mathrm{S_T}}\cdot\mathbf{n} = 0$ since by its definition [see Eq. (47)] $\mathbf{n} = \frac{J^i}{J_{\mathrm{s}}}\mathbf{G}^{i\,\mathrm{T}}\mathbf{N}$, and since $\mathbf{V}_{\mathrm{S_T}}\cdot\mathbf{N} = 0$. Thus, the quantity $\mathbf{F}\mathbf{V}_{\mathrm{S_T}}$ is tangential to the interface. Therefore, using Eq. (109), we obtain

$$V_{\mathrm{S_N}} = \frac{J_{\mathrm{s}}}{J^i}(\mathbf{v}_{\mathrm{s}} - \mathbf{v}^i)\cdot\mathbf{n} \tag{49}$$

$$\mathbf{F}^i\mathbf{V}_{\mathrm{S_T}} = \mathbf{P}(\mathbf{v}_{\mathrm{s}} - \mathbf{v}^i) \tag{50}$$

This last quantity $\mathbf{P}(\mathbf{v}_{\mathrm{s}} - \mathbf{v}^i)$ is the difference in velocity in the tangential direction between the interface and the neighboring material point. Using the definition of the first Piola–Kirchhoff stress [Eq. (124)] $\boldsymbol{\sigma}_{\mathrm{I}}\mathbf{N} = J_{\mathrm{s}}\boldsymbol{\sigma}\mathbf{n}$, we can now write the first term in Eq. (46) as

$$\mathbf{F}^i\mathbf{V}_{\mathrm{S_T}}\cdot\boldsymbol{\sigma}_{\mathrm{I}}\mathbf{N} = J_{\mathrm{s}}\mathbf{P}(\mathbf{v}_{\mathrm{s}} - \mathbf{v}^i)\cdot\boldsymbol{\sigma}\mathbf{n} \tag{51}$$

The right-hand side is zero if there is no slip in the tangential direction between the surface and the adjacent material point, that is, if $\mathbf{P}\,(\mathbf{v}_{\mathrm{s}} - \mathbf{v}) = 0$.

Now, treating the dissipation due to tangential slip independent of the normal velocity causing the growth, the thermodynamic second law conditions for growth, Eq. (46), may be stated as:

$$V_{\mathrm{S_N}} \mathbf{N} \cdot [\![\Sigma_\nu - \boldsymbol{\sigma}_{\mathrm{I}}]\!] \mathbf{N} \geq 0 \quad \text{on } \Gamma_{\mathrm{s}0} \tag{52}$$

$$-\mathbf{V}_{\mathbf{S_T}} \cdot \left[\!\!\left[\mathbf{F}^{\mathrm{T}} \boldsymbol{\sigma}_{\mathrm{I}} \right]\!\!\right] \mathbf{N} \geq 0 \quad \text{on } \Gamma_{\mathrm{s}0} \tag{53}$$

with $\mathbf{N} \cdot [\![\Sigma_\nu - \boldsymbol{\sigma}_{\mathrm{I}}]\!] \mathbf{N}$ representing a jump in volumetric energy density. The second condition is trivially satisfied in the absence of slip.

Recalling that the positive normal velocity points in the direction $\mathbf{N}$ of the interface, from the $-$ Phase to the $+$ Phase in the reference configuration, we will assume a convention that Phase $-$ is the growing phase and therefore, $V_{\mathrm{S_N}}$ is positive during the growth. Although it is not necessary to choose a priori the observed quantity, we choose the surface normal speed $V_{\mathrm{S_N}}$ as a macroscopic, positive observed quantity. Therefore, we restate Eqs. (52) and (53) to require that:

$$\mathbf{N} \cdot [\![\Sigma_\nu - \boldsymbol{\sigma}_{\mathrm{I}}]\!] \mathbf{N} \geq 0 \quad \text{on } \Gamma_{\mathrm{s}0} \tag{54}$$

$$V_{\mathrm{S_N}} = C_{V_N} \mathbf{N} \cdot [\![\Sigma_\nu - \boldsymbol{\sigma}_{\mathrm{I}}]\!] \mathbf{N} \quad \text{on } \Gamma_{\mathrm{s}0} \tag{55}$$

$$\mathbf{V}_{\mathbf{S_T}} = -C_{V_T} \left[\!\!\left[\mathbf{F}^{\mathrm{T}} \boldsymbol{\sigma}_{\mathrm{I}} \right]\!\!\right] \mathbf{N} \quad \text{on } \Gamma_{\mathrm{s}0} \tag{56}$$

where C_{V_N} and C_{V_T} are arbitrary positive quantities.

4.1 Growth conditions in the current configuration

In this section, we derive an alternative form of Eq. (54) in the current configuration. Using Eq. (124) in the interface momentum balance equation Eq. (23), ignoring inertial effects, one can write

$$\begin{aligned} [\![\boldsymbol{\sigma}_{\mathrm{I}}]\!] \mathbf{N} \mathrm{d}\Gamma_{\mathrm{s}0} &= -\nabla_{\mathrm{s}} \cdot (\mathbf{P} \boldsymbol{\sigma}_{\mathrm{s}}) \, \mathrm{d}\Gamma_{\mathrm{s}} \\ &= -\left(\kappa \boldsymbol{\sigma}_{\mathrm{s}} \mathbf{n} + \nabla_{\mathrm{s}} \cdot \boldsymbol{\sigma}_{\mathrm{s}} \right) J_{\mathrm{s}} \mathrm{d}\Gamma_{\mathrm{s}0} \end{aligned} \tag{57}$$

Substituting Eqs. (57) into (54), and utilizing Eqs. (47) and (48), we get

$$\frac{1}{J_{\mathrm{s}}} \mathbf{N} \cdot [\![\Sigma_\nu]\!] \mathbf{N} + \frac{\mathbf{F}^{\mathrm{T}} \mathbf{n}}{\sqrt{\mathbf{n} \cdot \mathbf{F} \mathbf{F}^{\mathrm{T}} \mathbf{n}}} \cdot \left(\kappa \boldsymbol{\sigma}_{\mathrm{s}} \mathbf{n} + \nabla_{\mathrm{s}} \cdot \boldsymbol{\sigma}_{\mathrm{s}} \right) \geq 0 \quad \text{on } \Gamma_{\mathrm{s}} \tag{58}$$

While the above equation is left in mixed form between current and reference configurations for ease of reading, it is possible to express the first term in the current configuration using Eqs. (48) and (125):

$$\frac{1}{J_{\mathrm{s}}} \mathbf{N} \cdot [\![\Sigma_\nu]\!] \mathbf{N} = \left[\!\!\left[\sqrt{\mathbf{n} \cdot \mathbf{F} \mathbf{F}^{\mathrm{T}} \mathbf{n}} \left(\rho \psi - \sum_{\alpha=1}^{N} \rho \mu^\alpha \nu^\alpha \right) - \frac{\mathbf{n} \cdot \mathbf{F} \left(\mathbf{F}^{\mathrm{T}} - \mathbf{I} \right) \boldsymbol{\sigma} \mathbf{n}}{\sqrt{\mathbf{n} \cdot \mathbf{F} \mathbf{F}^{\mathrm{T}} \mathbf{n}}} \right]\!\!\right] \tag{59}$$

Similar to the above derivation, we can derive the following condition using Eqs. (50) and (51):

$$\left[\!\!\left[\mathbf{F}^{\mathrm{T}} \boldsymbol{\sigma}_{\mathrm{I}} \right]\!\!\right] \mathbf{N} = J_{\mathrm{s}} \left[\!\!\left[\mathbf{F}^{\mathrm{T}} \boldsymbol{\sigma} \right]\!\!\right] \mathbf{n} \quad \text{on } \Gamma_{\mathrm{s}0} \tag{60}$$

Thus, utilizing Eq. (50), we can write the second law condition of Eq. (53) in the current configuration as

$$-\mathbf{P}(\mathbf{v}_{\mathrm{s}} - \mathbf{v}^{i}) \cdot \mathbf{G}^{i\mathrm{T}} \left[\!\!\left[\mathbf{F}^{\mathrm{T}} \boldsymbol{\sigma} \right]\!\!\right] \mathbf{n} \geq 0 \quad \text{on } \Gamma_{\mathrm{s}} \tag{61}$$

Substituting Eq. (59) into the growth condition into Eq. (58), we get the current configuration forms of Eqs. (54) and (55):

$$g_{sn} \equiv \left[\!\left[\sqrt{\mathbf{n}\cdot\mathbf{F}\mathbf{F}^{\mathrm{T}}\mathbf{n}} \left(\rho\psi - \sum_{\alpha=1}^{N} \rho\mu^{\alpha}\nu^{\alpha} \right) - \frac{\mathbf{n}\cdot\mathbf{F}\left(\mathbf{F}^{\mathrm{T}}-\mathbf{I}\right)\boldsymbol{\sigma}\mathbf{n}}{\sqrt{\mathbf{n}\cdot\mathbf{F}\mathbf{F}^{\mathrm{T}}\mathbf{n}}} \right]\!\right] + \frac{\mathbf{F}^{\mathrm{T}}\mathbf{n}}{\sqrt{\mathbf{n}\cdot\mathbf{F}\mathbf{F}^{\mathrm{T}}\mathbf{n}}} \cdot \left(\kappa\boldsymbol{\sigma}_{\mathrm{s}}\mathbf{n} + \nabla_{\mathrm{s}}\cdot\boldsymbol{\sigma}_{\mathrm{s}}\right) \geq 0 \quad \text{on } \Gamma_{\mathrm{s}} \tag{62}$$

$$(\mathbf{v}_{\mathrm{s}} - \mathbf{v}^{i})\cdot\mathbf{n} = c_{v_n} J^{i} g_{sn} \quad \text{on } \Gamma_{\mathrm{s}} \tag{63}$$

$$\mathbf{P}(\mathbf{v}_{\mathrm{s}} - \mathbf{v}^{i}) = -c_{v_t}\mathbf{G}^{i\mathrm{T}} \left[\!\left[\mathbf{F}^{\mathrm{T}}\boldsymbol{\sigma} \right]\!\right] \mathbf{n} \quad \text{on } \Gamma_{\mathrm{s}} \tag{64}$$

where we have used Eqs. (49) and (61) to arrive at the above conditions. c_{v_n} and c_{v_t} are arbitrary, positive proportionality constants.

4.2 Statistical growth condition

In general, the atomistic phenomena that lead to phase nucleation and growth are statistical in nature. Thus, in experimental observations, the growth condition of Eq. (54) requires a treatment keeping in mind the inherent variability at microscopic length scales. Considering now Eq. (62), the alternative form of Eq. (54), we rewrite the equation as

$$g_{sn} \equiv \left(H - \frac{G}{l} \right) \geq 0 \quad \text{on } \Gamma_{\mathrm{s}_0} \tag{65}$$

where H and G are volumetric and surface energy densities, respectively, and l is a characteristic length scale in the current configuration as explained below. The definitions of H and G follow from Eq. (62)

$$H\left(\mathbf{F}, \nu^{\alpha}, T\right) = \left[\!\left[\sqrt{\mathbf{n}\cdot\mathbf{F}\mathbf{F}^{\mathrm{T}}\mathbf{n}} \left(\rho\psi - \sum_{\alpha=1}^{N} \rho\mu^{\alpha}\nu^{\alpha} \right) - \frac{\mathbf{n}\cdot\mathbf{F}\left(\mathbf{F}^{\mathrm{T}}-\mathbf{I}\right)\boldsymbol{\sigma}\mathbf{n}}{\sqrt{\mathbf{n}\cdot\mathbf{F}\mathbf{F}^{\mathrm{T}}\mathbf{n}}} \right]\!\right] \tag{66}$$

$$G\left(\mathbf{F}, \boldsymbol{\sigma}_{\mathrm{s}}, T\right) = -l \frac{\mathbf{F}^{\mathrm{T}}\mathbf{n}}{\sqrt{\mathbf{n}\cdot\mathbf{F}\mathbf{F}^{\mathrm{T}}\mathbf{n}}} \cdot \left(\kappa\boldsymbol{\sigma}_{\mathrm{s}}\mathbf{n} + \nabla_{\mathrm{s}}\cdot\boldsymbol{\sigma}_{\mathrm{s}}\right) \tag{67}$$

The arguments in the above expressions explicitly indicate the independent physical variables that influence the quantities. For ease of reading, henceforth, we will not explicitly include the arguments when referring to these quantities. The explicit introduction of the length scale l in the definition of G nullifies the length scale dependence inherent in the expression on the right in Eq. (62) due to the curvature and surface divergence terms.

Since, for an applied configurational force, the observed velocity in general is influenced by microstructural arrangement influenced by atomic scale uncertainty, we now consider a probabilistic treatment of the observed velocity for a given (deterministic) configurational force. A natural choice for the probabilistic distribution that captures the atomic uncertainty in $\left(v_{\mathrm{s_n}} - v_n\right)$ is the Boltzmann distribution [41]. Therefore, we define the probability density function for $\left(v_{\mathrm{s_n}} - v_n\right)$ as

$$f\left(v_{\mathrm{s_n}} - v_n\right) \equiv f\left(c_{\mathrm{E}}\right) = f_0 \exp\left[-\left(\frac{c_{\mathrm{E}} g_{sn} l^3}{k_{\mathrm{B}} T} \right) \right] \tag{68}$$

where k_{B} is the Boltzmann constant, l is a characteristic length in the current configuration, and c_{E} is a positive non-dimensional measure that captures the uncertainty in the energy causing the interface motion. The unknown f_0 is evaluated by using the property of the probability density function

$$\int_0^{\infty} f\left(c_{\mathrm{E}}\right) \mathrm{d}c_{\mathrm{E}} = 1 \rightarrow f_0 = \frac{g_{sn} l^3}{k_{\mathrm{B}} T} \tag{69}$$

where we have used the physical requirement that $g_{sn}, l > 0$. We now define a positive energy quantity E for ease of recognition, which is dimensionally of the form:

$$E = c_{\mathrm{E}} g_{sn} l^3 \tag{70}$$

Finally, assuming the existence of a critical value of the energy E_{c}, the expected surface velocity resulting from the second law condition of Eq. (63) is:

$$\begin{aligned}\left\langle v_{\mathrm{S_n}} - v_n^i \right\rangle &= \int_{E_{\mathrm{c}}}^{\infty} (v_{\mathrm{S_n}} - v_n^i) f(E) \mathrm{d}E \\ &= c_{v_n} J^i g_{sn} \exp\left[- \left(\frac{E_{\mathrm{c}}}{k_{\mathrm{B}} T} \right) \right]\end{aligned} \tag{71}$$

with g_{sn} as defined in Eqs. (62) and (65). The corresponding form in the reference configuration is

$$\left\langle V_{\mathrm{S_N}} \right\rangle = C_{V_N} \left(\mathbf{N} \cdot [\![\Sigma_\nu - \boldsymbol{\sigma}_{\mathrm{I}}]\!] \mathbf{N} \right) \exp\left[- \left(\frac{E_{\mathrm{c}}}{k_{\mathrm{B}} T} \right) \right] \tag{72}$$

4.3 Application to small deformation diffusive void growth

Assuming small deformation from the definition of surface jacobian Eq. (48) we have,

$$\begin{aligned}\frac{J}{J_{\mathrm{s}}} &= \sqrt{\mathbf{n} \cdot \mathbf{F}\mathbf{F}^T \mathbf{n}} \\ &= \sqrt{\mathbf{n} \cdot (\mathbf{I} + \nabla \mathbf{u}^T)(\mathbf{I} + \nabla \mathbf{u}) \mathbf{n}} \\ &\approx \sqrt{\mathbf{n} \cdot (\mathbf{I} + \nabla \mathbf{u}^T + \nabla \mathbf{u}) \mathbf{n}} \\ \frac{J}{J_{\mathrm{s}}} &\approx \sqrt{1 + 2\varepsilon_{nn}}\end{aligned} \tag{73}$$

where $\boldsymbol{\varepsilon} = \frac{1}{2} \left(\nabla \mathbf{u} + \nabla \mathbf{u}^T \right)$ is the infinitesimal strain tensor, $\varepsilon_{nn} = \mathbf{n} \cdot \boldsymbol{\varepsilon} \mathbf{n}$ is the normal strain, and the quadratic terms of $\nabla \mathbf{u}$ are assumed to be negligible. We can now simplify Eq. (59) under assumptions of small deformations:

$$\begin{aligned}\frac{1}{J_{\mathrm{s}}} \mathbf{N} \cdot [\![\Sigma_\nu]\!] \mathbf{N} &= \left[\!\!\left[\sqrt{\mathbf{n} \cdot \mathbf{F}\mathbf{F}^{\mathrm{T}} \mathbf{n}} \left(\rho\psi - \sum_{\alpha=1}^{N} \rho \mu^\alpha \nu^\alpha \right) - \frac{\mathbf{n} \cdot \mathbf{F} \left(\mathbf{F}^{\mathrm{T}} - \mathbf{I} \right) \boldsymbol{\sigma} \mathbf{n}}{\sqrt{\mathbf{n} \cdot \mathbf{F}\mathbf{F}^{\mathrm{T}} \mathbf{n}}} \right]\!\!\right] \\ &\approx \left[\!\!\left[\sqrt{1 + 2\varepsilon_{nn}} \left(\rho\psi - \sum_{\alpha=1}^{N} \rho \mu^\alpha \nu^\alpha \right) - \frac{1}{\sqrt{1 + 2\varepsilon_{nn}}} \mathbf{n} \cdot \nabla \mathbf{u} \boldsymbol{\sigma} \mathbf{n} \right]\!\!\right] \\ &\approx \left[\!\!\left[\left(\rho\psi - \sum_{\alpha=1}^{N} \rho \mu^\alpha \nu^\alpha \right) - \mathbf{n} \cdot \nabla \mathbf{u} \boldsymbol{\sigma} \mathbf{n} \right]\!\!\right] \\ &\approx \left[\!\!\left[\mathbf{n} \cdot \Sigma \mathbf{n} - \sum_{\alpha=1}^{N} \rho \mu^\alpha \nu^\alpha \right]\!\!\right]\end{aligned} \tag{74}$$

where we have used the simplification $\mathbf{F}(\mathbf{F}^T - \mathbf{I}) = \mathbf{F}\mathbf{F}^T - \mathbf{F} \approx \mathbf{I} + \nabla \mathbf{u}^T + \nabla \mathbf{u} - (\mathbf{I} + \nabla \mathbf{u}^T) = \nabla \mathbf{u}$, and the small strain assumption, $\varepsilon_{nn} \ll 1$. Σ is the Eshelby energy–momentum tensor defined as $\Sigma = \rho\psi \mathbf{I} - \nabla \mathbf{u} \boldsymbol{\sigma}$. This reduces the growth condition of Eq. (58) to,

$$\begin{aligned}\left[\!\!\left[\mathbf{n} \cdot \Sigma \mathbf{n} - \sum_{\alpha=1}^{N} \rho \mu^\alpha \nu^\alpha \right]\!\!\right] &\geq - \frac{\mathbf{F}^{\mathrm{T}} \mathbf{n}}{\sqrt{\mathbf{n} \cdot \mathbf{F}\mathbf{F}^{\mathrm{T}} \mathbf{n}}} \cdot (\kappa \boldsymbol{\sigma}_{\mathrm{s}} \mathbf{n} + \nabla_{\mathrm{s}} \cdot \boldsymbol{\sigma}_{\mathrm{s}}) \\ &\geq - \frac{1}{\sqrt{1 + 2\varepsilon_{nn}}} (\mathbf{I} + \nabla \mathbf{u}) \mathbf{n} \cdot (\kappa \boldsymbol{\sigma}_{\mathrm{s}} \mathbf{n} + \nabla_{\mathrm{s}} \cdot \boldsymbol{\sigma}_{\mathrm{s}})\end{aligned} \tag{75}$$

Now, if the surface stress is homogeneous and isotropic ($\boldsymbol{\sigma}_{\mathrm{s}} = \gamma \mathbf{I}$), and if strains are small $\varepsilon_{nn} \ll 1$, the above equation simplifies to,

$$\left\llbracket \mathbf{n}\cdot\Sigma\mathbf{n}-\sum_{\alpha=1}^{N}\rho\mu^{\alpha}\nu^{\alpha}\right\rrbracket+\kappa\gamma\geq 0 \quad \text{on } \varGamma_{\mathrm{s}} \tag{76}$$

Now, a growing phase is locally required to have negative curvature. Thus, we define a local radius of curvature $r=-\frac{1}{\kappa}>0$, and assuming Phase $-$ to be void (values are zero inside the jump term), we get the condition for diffusive void growth as

$$\mathbf{n}\cdot\Sigma\mathbf{n}-\sum_{\alpha=1}^{N}\rho\mu^{\alpha}\nu^{\alpha}-\frac{\gamma}{r}\geq 0 \quad \text{on } \varGamma_{\mathrm{s}} \tag{77}$$

Finally, applying the statistical arguments of Sect. 4.2, we arrive at the small deformation diffusive void normal velocity as:

$$v_{\mathrm{s_n}}=c_{v_n}\left(\mathbf{n}\cdot\Sigma\mathbf{n}-\sum_{\alpha=1}^{N}\rho\mu^{\alpha}\nu^{\alpha}-\frac{\gamma}{r}\right)\exp\left[-\left(\frac{E_{\mathrm{c}}}{k_{\mathrm{B}}T}\right)\right]. \tag{78}$$

5 Criterion for phase nucleation

We model the nucleation of a new phase as the growth of an infinitesimally small embryo under the influence of the various thermodynamic forces. The uncertainty, however, is presumed to occur in the length scale l in Eq. (68). Consider an infinitesimal nucleus of $\varOmega_n=l^3$, with the bounding surface $\varGamma_n$. During nucleation, for a supplied energy density, the resulting length scale l is presumed uncertain and thus, only some nuclei will continue to grow into the second phase. That is, the configurational force g_{sn} is deterministic, while the characteristic volume is uncertain. Thus,

$$l\geq l_{\mathrm{c}} \tag{79}$$

with the critical length defined as $l_{\mathrm{c}}=\frac{G}{H}$, $G\geq 0$, $H>0$. During nucleation, it is expected that the length scale $l\ll 1$. Therefore, the length scale uncertainty that expresses through energy that varies as l^2 dominates over the energy that varies as l^3. Thus, representing the energy that varies as l^2 as $c_G Gl^2$ $(G>0)$ with c_G an unknown positive constant, the uncertainty in l may be expressed using the Boltzmann distribution as

$$f(l)=f_0\exp\left[-\left(\frac{c_G Gl^2}{k_{\mathrm{B}}T}\right)\right] \tag{80}$$

The required condition for nucleation is then written as the probability that the length l will exceed the critical value l_{c}:

$$\begin{aligned} P(l>l_{\mathrm{c}}) &= \int_{l_{\mathrm{c}}}^{\infty} f(l)\mathrm{d}l \\ &= 1-\operatorname{erf}\left[\sqrt{\frac{c_G G^3}{k_{\mathrm{B}}T}}\frac{1}{H}\right] \\ &= 1-\operatorname{erf}\left[\frac{\hat{H}_{\mathrm{c}}}{H}\right] \end{aligned} \tag{81}$$

with the definition $\hat{H}_{\mathrm{c}}=\sqrt{\frac{c_G G^3}{k_{\mathrm{B}}T}}$. $\hat{H}_{\mathrm{c}}$ is a theoretical estimate of the characteristic value of H at which nucleation will accelerate, with $\operatorname{erf}(x)$ being the error function. It is interesting to note the nonlinear dependence of the characteristic value $\hat{H}_{\mathrm{c}}$ on the surface stress on the interface. A plot of the probability of nucleation against normalized H is shown in Fig. 3. It is clear from the figure that the probability of nucleation is practically zero if $H\leq H_{\mathrm{c}}$. A one percent change in the probability value occurs when $H\approx 0.55\hat{H}_{\mathrm{c}}$.

The existence of a critical value beyond which nucleation occurs rapidly is supported experimentally [42,43]. While the value of H_{c} can be estimated theoretically as in the $\hat{H}_{\mathrm{c}}$ value, in general, the theoretical estimate may not correlate well with experimental observation due to errors in estimating the surface energy. The surface energy of a highly curved interface will be different from the bulk surface energy calculated for a flat surface. Thus, the value of H_{c} would in general be estimated experimentally. Finally, in the event $l_{\mathrm{c}}=G=0$, then, trivially, the probability $P(l>l_{\mathrm{c}})=1$.

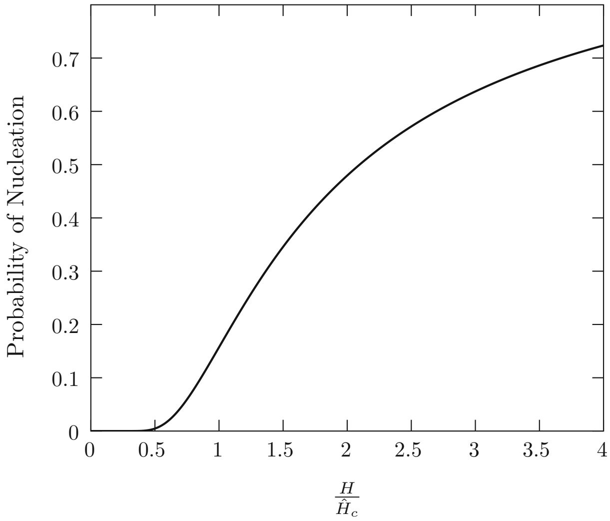

Fig. 3 Probability of nucleation versus $\frac{H}{\hat{H}_c}$. There is a sharp increase in the probability of nucleation beyond a characteristic value $H \geq H_c$. A one percent change in the probability value occurs when $H \approx 0.55\hat{H}_c$

5.1 Reduction to classical nucleation condition

In classical nucleation, the deformation and stress in the bulk are assumed negligible (pure diffusion) and that surface stress is isotropic ($\boldsymbol{\sigma}_s = \gamma \mathbf{I}$), leading to $G = -l\kappa\gamma$. A growing nucleus of Phase − will have a negative total curvature; therefore, in Eq. (76), we consider $r_n = -\frac{1}{\kappa}$ as a characteristic radius of the growing nucleus in the current configuration. This gives $G = \gamma$. For a viable nucleus, the right-hand side of Eq. (76) has to be positive. Thus, Eq. (65) reduces to

$$r_n \geq \frac{\gamma}{H} \tag{82}$$

where

$$H = \left[\!\left[\rho\psi - \sum_{\alpha=1}^{N} \rho\mu^\alpha \nu^\alpha \right]\!\right] \tag{83}$$

H is the (deterministic) volumetric energy density for the growth of the nucleus. Specifically for a sphere, the length scale is $r_n = \frac{R}{2}$, where R is the radius of the sphere. The above criterion describes the minimum radius in the current configuration for viable nucleation in the presence of isotropic surface stress.

The classical nucleation theory [44,45] suggests that when embryos of the new phase are too small to satisfy Eq. (82), they are unstable and collapse. Embryos above the critical size undergo stable growth to form viable nuclei. Since the embryos are very small, the energy of formation is predominantly the surface energy, varying as $G_n \approx c_\gamma \gamma r_n^2$, where c_γ is a positive constant relating the defined length scale to the surface area. For a sphere, $c_\gamma = 16\pi$. Following the procedure of the previous section, the probability of nucleation then is

$$P\left(r_n \geq \frac{\gamma}{H}\right) = 1 - \operatorname{erf}\left(\frac{\hat{H}_c}{H}\right) \tag{84}$$

where $\hat{H}_c = \sqrt{\frac{c_\gamma \gamma^3}{k_B T}}$. The classical nucleation theory is thus a special case of the general criterion of Eq. (81).

6 Electromigration-induced void nucleation and growth

In the context of entropic inequality, the applied electrical field provides an external power to each diffusing species of the form $\boldsymbol{j}^\alpha \cdot \boldsymbol{e}^\alpha$ leading to modification of the constitutive equation for the bulk mass flux, Eq. (14),

$$\boldsymbol{j}^\alpha = -\mathbf{M}^\alpha(\nabla\mu^\alpha + \boldsymbol{e}^\alpha) \quad \forall\alpha \tag{85}$$

Since the free energy is a function of only the deformation gradient, temperature and concentration, it is unaffected by the presence of the electromigration force. Similarly, the electrical field may be thought to add an external surface power term $\boldsymbol{h}_{\mathbf{t}}^{\alpha} \cdot \boldsymbol{e}_{\mathrm{s}}^{\alpha}$ leading to the modification of the surface constitutive equation, Eq. (41),

$$\boldsymbol{h}_{\mathbf{t}}^{\alpha} = -\mathbf{M}_{\mathrm{s}}^{\alpha}(\nabla \mu_{\mathrm{s}}^{\alpha} + \boldsymbol{e}_{\mathrm{s}}^{\alpha}) \quad \forall \alpha \tag{86}$$

Since electromigration force causes a contribution only to the external power, the criterion for nucleation, Eq. (84), remains unchanged. However, since the interface is now between a void phase and a solid phase, the nucleation criterion simplifies to:

$$\rho\psi - \sum_{\alpha=1}^{N} \rho\mu^{\alpha}\nu^{\alpha} \geq H_{\mathrm{c}} \tag{87}$$

where all the quantities are evaluated in the solid phase.

The experiments by Lane et al. [16] may now be interpreted in light of Eq. (87) as follows. The dominant path for the diffusion in copper is along the grain boundaries. Therefore, for a copper line subject to electromigration force, the vacancy concentration at the cathode at a given time instant is independent of the adhesion energy of the interface (between the metal and barrier layer) binding the line. As the vacancy concentration increases at the cathode, the hydrostatic stress will also increase, and consequently, there is an increase in the chemical potential and therefore H near the cathode. When H reaches a critical value, H_{c}, which depends on the adhesion energy of the interface, a void will nucleate. Once a void nucleates, the growth of the void is governed by the magnitude of the configurational force at the interface. Since κ is negative for a convex void, the force is greater when the adhesion energy is smaller, and the void will grow at a faster rate at an interface with lower adhesion energy compared to one with a stronger adhesion.

7 Application: critical energy density of Al–TiN interface

In this section, we simulate the famous Blech's experiment [46] to estimate the critical value of (H_{c}) for Al–TiN interface. Figure 4 shows a schematic of the geometry used in Blech's experiment. The experiment consisted of a current-carrying aluminum line deposited on a titanium nitride (TiN) layer. The ends of the TiN layer were connected to the electrical leads. Thus, the current enters the geometry through the TiN layer, passes through the Al line (due to the lower resistivity) and then exits once again through the TiN layer. From a historical perspective, this experiment is important because it elucidates the mechanism behind electromigration. Specifically, Blech identified a critical length of the interconnect line, for a given current density, now called the Blech length, below which no electromigration was observed. Furthermore, he observed that the product of the critical length and the current density was a constant. He then explained the observations by developing a model for how the vacancy concentration gradient in the line setup by the initial electromigration can balance the forced diffusion due to the electric current. When the vacancy concentration at the cathode is below a critical limit, electromigration voids are not observed.

We show that using the notion of the Blech length, one can estimate the value of H_{c}. This then provides an easy method to determine void nucleation criterion in metals. Figure 5 shows a portion of the geometry that was used to simulate Blech's experiment. The length of the Al line was chosen to be equal to 10 μm. The interface between Al and TiN was modeled as a distinct material with thickness equal to 0.1 μm but with higher diffusivity (see Table 1). It is known from Blech's experiments that for Al tested in a geometry of this type, the critical value of jL was equal to $(jL)_c = 1260$ A/cm. In order to simulate electromigration, it is necessary

Fig. 4 Schematic of the Blech structure that was used in the simulation

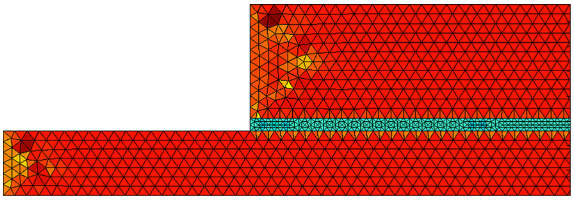

Fig. 5 Mesh of the Blech structure with the color representing the size of the elements

Table 1 Table of material properties

Material property	Value
Aluminum diffusivity	$1 \times 10^{-14}\ \mathrm{m}^2/\mathrm{s}$
Interface diffusivity	$1 \times 10^{-}6\,\mathrm{m}^2/\mathrm{s}$
Al Young's modulus	70×10^9 Pa
TiN Young's Modulus	500×10^9 Pa
Al electrical conductivity	3.774×10^7 S/m
TiN electrical conductivity	2.6×10^4 S/m

to simultaneously solve three sets of partial differential equations [10,12]: (1) the electrical charge continuity equation, (2) the vacancy diffusion equation and (3) the stress–equilibrium equation and the coupling between them. The stress problem was solved by modifying the elastic constitutive behavior of Al to account for the dilational strain that is induced due to vacancy concentration variations. Electromigration was modeled by solving an advection–diffusion equation over the Al and interface domains. Diffusion was not simulated in the TiN region, as it is known to be resistant to electromigration.

The electrical boundary conditions in the simulations were as shown in Fig. 4. The electric potential was applied at the ends of TiN layer corresponding to the critical current density, $(jL)_c$. All the boundaries were made impervious to vacancy diffusion during the simulations. The initial vacancy concentration was assumed to be 0.9 mol/m^3 roughly corresponding to a concentration of 1 vacancy for every 10^6 atoms of copper. All the boundaries were held fixed during the elastic stress analysis. The line was assumed to be initially stress-free.

Figure 6 shows the variation of H at the cathode end as a function of time. The onset of electromigration equilibrium occurs when $t \approx 15{,}000$ s. Figure 7 shows the spatial variation of several physical variables in the Blech structure once vacancy concentration equilibrium was achieved. Figure 7a shows the electrical current density, $\boldsymbol{j} = \sigma \nabla \phi$, where ϕ is the electrical potential and the σ is the electrical conductivity. Since the conductivity is higher in Al compared to TiN, the current density is correspondingly higher. Figure 7b shows the distribution of vacancy concentration. As might be expected, the vacancy concentration is higher at the

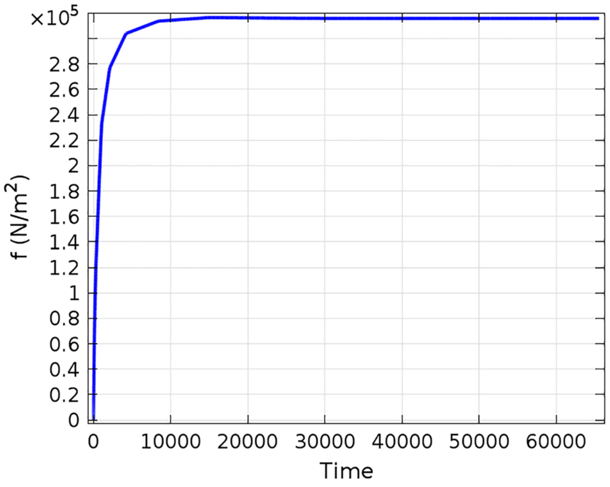

Fig. 6 Variation of H at the cathode as a function of time

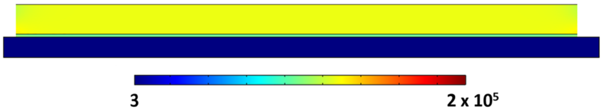

(a) Electrical current density (A/cm^2)

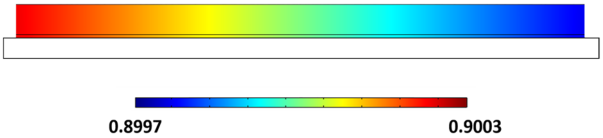

(b) Vacancy concentration (moles/m^3)

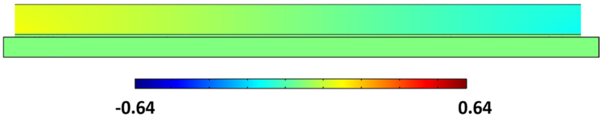

(c) Hydrostatic stress (MPa)

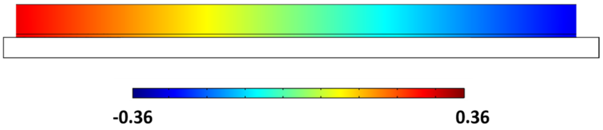

(d) H (Joules/cm^3)

Fig. 7 Spatial variation of the various physical quantities at equilibrium

cathode than at the anode. Consequently, the hydrostatic stress is tensile at the cathode and compressive at the anode. Due to the higher vacancy concentration and the tensile hydrostatic stress, H is also higher at the cathode. Since it is known that it is at this value of H that voids begin to nucleate at the cathode, this H is equal to H_c. Hence, the Blech experiment may be used to determine the value of H_c to predict void nucleation in a material.

The simulations indicate that the value of $H_c = 5.5$ Joules/cm^3 for the Al–TiN interface. The value of H_c being an intrinsic property of the interface, it does not depend on the diffusivities of the materials in the test structure. But, to accurately predict the time for void nucleation, the diffusivities through the bulk, grain boundaries and through the metal–dielectric interfaces will need to be known. In general, as in fracture mechanics, in a structure with multiple interfaces, the knowledge of H alone is insufficient to predict void location since the critical value of H_c depends on the specific interface.

8 Concluding remarks

In this paper, we derived the balance laws at a moving interface, analogous to those in the bulk. The free energy inequality on a moving interface naturally yields: (1) constitutive equations relating surface free energy to the surface stress, (2) surface entropy to the surface free energy, (3) constitutive equation relating surface species mass flux to the gradient of surface chemical potential and (4) surface heat flux to the gradient of surface temperature, respectively. The derived interface second law condition was shown to lead to a configurational force associated with the interface evolution that naturally extends the Eshelby energy–momentum tensor to problems with species diffusion. Also, the dependence on the jump in the free energy and the elastic misfit energy are shown to emerge naturally from the thermodynamic restrictions at the interface. This configurational force was then used to develop the criteria for growth and nucleation of a phase in a body with multiple diffusing species undergoing finite deformation, and with arbitrary surface stress. The interface growth and nucleation criteria developed in the present paper are thermodynamic restrictions and as such do not presuppose any constitutive relation for the bulk or surface diffusional flux. The phase growth condition is statistical to account for the statistical nature of the atomistic phenomena that lead to phase growth. Conditions for small deformation diffusive void growth as well as the classical nucleation theory are obtained as special cases of the developed general criteria for growth and nucleation, respectively. It is shown that a critical material-dependent energy density that must be overcome for nucleation (H_c) naturally arises as a consequence of the statistical distribution of nucleus sizes, and the existence of a critical nucleus size. As an application, the developed theory is used to study inherent material resistance to void nucleation at Al–TiN interface. Through a simulation of Blech's experiments, the critical energy density for the interface is estimated as $H_c = 5.5\,\text{Joules/cm}^3$.

Acknowledgements This study was partially supported by Intel Corporation and the Semiconductor Research Corporation under Task 1292.090.

A Surface identities

Following the definitions given in [37], the surface gradient is defined using the projection tensor:

$$\mathbf{P} = \mathbf{I} - \mathbf{n} \otimes \mathbf{n} \tag{88}$$

where $\mathbf{I}$ is the identity tensor and $\mathbf{n}$ is the normal to the surface at the point of interest. Referring to Fig. 2, for a scalar field $\phi_s(\mathbf{x}_s)$ defined on the subregion Γ_s of Γ, the surface gradient operator is defined to relate the gradient of the field in its extension into the body as

$$\nabla_s \phi_s = \mathbf{P}\nabla\phi_s \tag{89}$$

where the quantity $\nabla_s \phi_s$ is defined on the tangent plane at the point of interest. Similarly, for a vector field $\mathbf{a}(\mathbf{x}_s)$ defined on the surface Γ_s, the surface gradient operator and the surface divergence operators are defined as

$$\nabla_s \mathbf{a} = \mathbf{P}\nabla\mathbf{a}, \quad \nabla_s \cdot \mathbf{a} = \operatorname{tr}(\nabla_s \mathbf{a}) = \mathbf{P} : \nabla\mathbf{a} \tag{90}$$

Finally, for a second-order tensor field $\mathbf{A}(\mathbf{x}_s)$ defined on Γ_s, the two surface operators are similarly defined as,

$$\nabla_s \mathbf{A} = \mathbf{P}\nabla\mathbf{A}, \quad \nabla_s \cdot \mathbf{A} = \operatorname{tr}(\nabla_s \mathbf{A}) = \mathbf{P} : \nabla\mathbf{A} \tag{91}$$

The curvature tensor at any point on the surface and the total curvature are defined using the surface gradient as

$$\mathbf{L} = -\nabla_s \mathbf{n}, \quad \kappa = \operatorname{tr}(\mathbf{L}) = -\nabla_s \cdot \mathbf{n} \tag{92}$$

where κ is the total curvature, or twice the mean value. The curvature tensor is fully tangential and symmetric. Further, from the above relationship, it is easy to show:

$$\nabla_s \cdot \mathbf{P} = \kappa\mathbf{n} \tag{93}$$

This gives a useful surface divergence product rule for any second-order tensor field $\mathbf{A}(\mathbf{x}_s)$,

$$\begin{aligned} \nabla_s \cdot (\mathbf{P}\mathbf{A}) &= (\nabla_s \cdot \mathbf{P}) \cdot \mathbf{A} + \mathbf{P} : \nabla\mathbf{A} \\ &= \kappa\mathbf{n} \cdot \mathbf{A} + \nabla_s \cdot \mathbf{A} \end{aligned} \tag{94}$$

We list next an identity that is useful for simplifications carried out in this paper. For smooth scalar and vector fields $\phi(\mathbf{x}_s)$ and $\mathbf{a}(\mathbf{x}_s)$, respectively,

$$\nabla_s \cdot \phi_s\mathbf{g} = \phi_s\nabla_s \cdot \mathbf{g} + \mathbf{g} \cdot \nabla_s \phi_s \tag{95}$$

The surface divergence theorem for a *tangential* vector field $\mathbf{a_t}(\mathbf{x}_s)$ defined on a subregion Γ_s is:

$$\int_{\Gamma_s} \nabla_s \cdot \mathbf{a_t}\, \mathrm{d}\Gamma_s = \oint_{\partial\Gamma_s} \mathbf{m} \cdot \mathbf{a_t}\, \mathrm{d}c \tag{96}$$

where $\mathbf{m}$ is tangent to the surface, but normal to the bounding curve $\partial \Gamma_\mathrm{s}$. For a *superficial* vector field with both normal and tangential components of the form $\mathbf{a} = a_n\mathbf{n} + \mathbf{a_t}$ such that $a_n = \mathbf{a}\cdot\mathbf{n}$, the above surface divergence theorem can be generalized using Eqs. (95) and (92) as

$$\int_{\Gamma_\mathrm{s}} \nabla_\mathrm{s} \cdot \mathbf{a}\,\mathrm{d}\Gamma_\mathrm{s} = -\int_{\Gamma_\mathrm{s}} \kappa\mathbf{n}\cdot\mathbf{a}\,\mathrm{d}\Gamma_\mathrm{s} + \oint_{\partial\Gamma_\mathrm{s}} \mathbf{m}\cdot\mathbf{a}\,\mathrm{d}c \tag{97}$$

Similarly for a *superficial* tensor field $\mathbf{A}(\mathbf{x}_\mathrm{s})$, the divergence theorem has the form,

$$\int_{\Gamma_\mathrm{s}} \nabla_\mathrm{s} \cdot \mathbf{A}\,\mathrm{d}\Gamma_\mathrm{s} = -\int_{\Gamma_\mathrm{s}} \kappa\mathbf{n}\cdot\mathbf{A}\,\mathrm{d}\Gamma_\mathrm{s} + \oint_{\partial\Gamma_\mathrm{s}} \mathbf{m}\cdot\mathbf{A}\,\mathrm{d}c \tag{98}$$

B Material time derivative of a bulk field

Given a field $\phi(\mathbf{x}, t)$, the material time derivative of the field is defined as [38]

$$\dot{\phi} = \frac{\partial\phi}{\partial t} + \mathbf{v}\cdot\nabla\phi \tag{99}$$

Thus,

$$\begin{aligned}\frac{\mathrm{d}}{\mathrm{d}t}\int_\Omega \phi\,\mathrm{d}\Omega &= \int_\Omega \dot{\phi}\,\mathrm{d}\Omega + \int_\Omega \phi\,\dot{\overline{\mathrm{d}\Omega}}\\ &= \int_\Omega \left(\frac{\partial\phi}{\partial t} + \mathbf{v}\cdot\nabla\phi\right)\mathrm{d}\Omega + \int_\Omega \phi\nabla\cdot\mathbf{v}\,\mathrm{d}\Omega\\ &= \int_\Omega \frac{\partial\phi}{\partial t}\,\mathrm{d}\Omega + \int_\Omega \nabla\cdot\phi\mathbf{v}\,\mathrm{d}\Omega\\ &= \int_\Omega \frac{\partial\phi}{\partial t}\,\mathrm{d}\Omega + \int_{\partial\Omega} \phi\mathbf{v}\cdot\mathbf{n}\,\mathrm{d}\Gamma_\mathrm{s}\end{aligned} \tag{100}$$

C Surface transport theorem

The surface transport theorem then gives the rate of change of a superficial scalar field, $\phi_\mathrm{s}(\mathbf{x}_\mathrm{s}(t), t)$, defined on the interface [47]. The surface transport theorem can be derived using the concept of material time derivative:

$$\frac{\mathrm{d}}{\mathrm{d}t}\int_{\Gamma_\mathrm{s}} \phi_\mathrm{s}\,\mathrm{d}\Gamma_\mathrm{s} = \int_{\Gamma_\mathrm{s}} \dot{\phi}_\mathrm{s}\,\mathrm{d}\Gamma_\mathrm{s} + \int_{\Gamma_\mathrm{s}} \phi_\mathrm{s}\,\dot{\overline{\mathrm{d}\Gamma_\mathrm{s}}} \tag{101}$$

By definition of material time derivative:

$$\dot{\phi}_\mathrm{s}\left(\mathbf{x}_\mathrm{s}(t), t\right) = \frac{\partial\phi_\mathrm{s}}{\partial t} + \frac{\partial\phi_\mathrm{s}}{\partial\mathbf{x}_\mathrm{s}}\cdot\frac{\mathrm{d}\mathbf{x}_\mathrm{s}}{\mathrm{d}t} \tag{102}$$

$$= \frac{\partial\phi_\mathrm{s}}{\partial t} + \mathbf{v}_\mathrm{s}\cdot\nabla\phi_\mathrm{s} \tag{103}$$

Now, the material time derivative of the differential surface element is [38]

$$\dot{\overline{\mathrm{d}\Gamma_\mathrm{s}}} = (\nabla\cdot\mathbf{v}_\mathrm{s} - \mathbf{n}\cdot\nabla\mathbf{v}_\mathrm{s}\mathbf{n})\,\mathrm{d}\Gamma_\mathrm{s} = \mathbf{P}:\nabla\mathbf{v}_\mathrm{s}\mathrm{d}\Gamma_\mathrm{s} = \nabla_\mathrm{s}\cdot\mathbf{v}_\mathrm{s}\mathrm{d}\Gamma_\mathrm{s} \tag{104}$$

Thus,

$$\frac{\mathrm{d}}{\mathrm{d}t}\int_{\Gamma_\mathrm{s}} \phi_\mathrm{s}\,\mathrm{d}\Gamma_\mathrm{s} = \int_{\Gamma_\mathrm{s}} \left(\dot{\phi}_\mathrm{s} + \phi_\mathrm{s}\nabla_\mathrm{s}\cdot\mathbf{v}_\mathrm{s}\right)\mathrm{d}\Gamma_\mathrm{s} \tag{105}$$

D Kinematics of a coherent interface

We begin with the usual definition of the velocity of a particle at a spatial location $\mathbf{x}\,(\mathbf{X}, t)$ obtained by holding position in the reference configuration, $\mathbf{X}$, fixed,

$$\mathbf{v} = \frac{\partial}{\partial t}\mathbf{x}\,(\mathbf{X}, t) \tag{106}$$

Now, we assume that the interface convects with the body and that different material particles come to occupy the interface at different instants of time. Hence, the interface can be viewed as evolving with time in both the reference and current configurations. Let $\mathbf{X}_\mathrm{S}\,(t)$ denote the reference coordinate of particles on the interface at time t. Then, the interface velocity as viewed in the reference configuration is given by [37],

$$\mathbf{V}_\mathrm{S} = \frac{\mathrm{d}}{\mathrm{d}t}\mathbf{X}_\mathrm{S}\,(t) \tag{107}$$

Similarly, the velocity of the interface in the current configuration is,

$$\begin{aligned}\mathbf{v}_\mathrm{s} &= \frac{\mathrm{d}}{\mathrm{d}t}\mathbf{x}_\mathrm{s}\,(\mathbf{X}_\mathrm{S}\,(t)\,,t) \\ &= \frac{\partial \mathbf{x}_\mathrm{s}}{\partial t} + \frac{\partial \mathbf{x}_\mathrm{s}}{\partial \mathbf{X}_\mathrm{S}}\cdot\frac{\mathrm{d}\mathbf{X}_\mathrm{S}}{\mathrm{d}t}\end{aligned} \tag{108}$$

The first term $\mathbf{v} = \frac{\partial \mathbf{x}_\mathrm{s}}{\partial t}$ represents the velocity of a material point currently at the interface, and $\mathbf{F} = \frac{\partial \mathbf{x}_\mathrm{s}}{\partial \mathbf{X}_\mathrm{S}}$ is the instantaneous deformation gradient at the spatial location $\mathbf{x}_\mathrm{s}$ with its corresponding reference location $\mathbf{X}_\mathrm{S}$. The subscripts on $\mathbf{x}_\mathrm{s}$ and $\mathbf{X}_\mathrm{S}$ in the definition of $\mathbf{F}$ serve to remind the fact that these material points currently reside on the interface, but are free to change in any direction. The second term represents the contribution due to interfacial motion in the reference configuration, since by Eq. (107), $\mathbf{V}_\mathrm{S} = \frac{\mathrm{d}\mathbf{X}_\mathrm{S}}{\mathrm{d}t}$ is the velocity of the interface in the reference configuration. Thus, the difference between the velocity of the interface and the velocity of a particle currently at the interface is,

$$\mathbf{v}_\mathrm{s} - \mathbf{v} = \mathbf{F}\mathbf{V}_\mathrm{S} \tag{109}$$

The inverse relationship is thus,

$$\mathbf{V}_\mathrm{S} = \mathbf{G}\,(\mathbf{v}_\mathrm{s} - \mathbf{v}) \tag{110}$$

where $\mathbf{G} = \mathbf{F}^{-1} = \frac{\partial \mathbf{X}_\mathrm{S}}{\partial \mathbf{x}_\mathrm{s}}$ is the inverse of the deformation gradient at a point on the interface. Furthermore, for a coherent interface, in both the reference and current configurations, at all times, the following conditions must be satisfied

$$\begin{aligned}[\![\mathbf{v}_\mathrm{s}]\!] &= 0 \\ [\![\mathbf{V}_\mathrm{S}]\!] &= 0\end{aligned} \tag{111}$$

This gives a relation for the jump in the bulk velocity across the interface,

$$[\![\mathbf{v}]\!] = -\,[\![\mathbf{v}_\mathrm{s} - \mathbf{v}]\!] = -\,[\![\mathbf{F}]\!]\,\mathbf{V}_\mathrm{S} \tag{112}$$

where we have used $[\![\mathbf{V}_\mathrm{S}]\!] = 0$. Although not done in the present paper, the above condition is sometimes further reduced by assuming that the deformation gradient jump is nonzero only in the normal direction [13]. That is,

$$[\![\mathbf{v}]\!] = -\,[\![\mathbf{F}]\!]\,\mathbf{N}V_{\mathrm{S_N}} \tag{113}$$

$$0 = -\,[\![\mathbf{F}]\!]\,\mathbf{V}_{\mathbf{S_T}} \tag{114}$$

where $V_{\mathrm{S_N}}$ is the normal component of the reference interface velocity, $V_{\mathrm{S_N}} = \mathbf{N}\cdot\mathbf{V}_\mathrm{S}$, and $\mathbf{V}_{\mathbf{S_T}}$ is the tangential component of the reference interface velocity.

The surface gradient and surface divergence of the interface velocity are next derived. Applying the surface gradient operation on Eq. (109), we get

$$\nabla_\mathrm{s}\,\mathbf{v}_\mathrm{s} = \mathbf{P}\nabla\mathbf{v} + \mathbf{P}\mathbf{G}^\mathrm{T}\left[\nabla_0\mathbf{F}\;\mathbf{V}_\mathrm{S} + \nabla_0\mathbf{V}_\mathrm{S}\;\mathbf{F}^\mathrm{T}\right] \tag{115}$$

Observing that $\frac{\partial}{\partial \mathbf{X}_\mathrm{S}}\left(\frac{\partial \mathbf{x}_\mathrm{s}}{\partial t}\right) = \frac{\partial}{\partial t}\left(\frac{\partial \mathbf{x}_\mathrm{s}}{\partial \mathbf{X}_\mathrm{S}}\right)$, the above expression can be rewritten as

$$\left(\nabla_\mathrm{s}\, \mathbf{v}_\mathrm{s}\right)^\mathrm{T} = \overset{\triangle}{\mathbf{F}}\mathbf{G}\mathbf{P} \tag{116}$$

where $\overset{\triangle}{\mathbf{F}}$ is the convected time derivative of the deformation gradient

$$\overset{\triangle}{\mathbf{F}} = \frac{\partial \mathbf{F}}{\partial t} + \left(\nabla_0 \mathbf{F}\ \mathbf{V}_\mathrm{S}\right)^\mathrm{T} + \mathbf{F}\ \left(\nabla_0 \mathbf{V}_\mathrm{S}\right)^\mathrm{T} \tag{117}$$

Finally, using the above derivation, it is easy to show that

$$\left(\nabla_\mathrm{s}\ \cdot \mathbf{v}_\mathrm{s}\right) = \overset{\triangle}{\mathbf{F}}\mathbf{G} : \mathbf{P} \tag{118}$$

E Derivation for the jump in stress–velocity term

Using Eq. (109), we write the stress–velocity jump term as

$$\llbracket \boldsymbol{\sigma}\, \mathbf{v} \rrbracket \cdot \mathbf{n} = \llbracket \boldsymbol{\sigma}\, \mathbf{v}_\mathrm{s} - \boldsymbol{\sigma}\ (\mathbf{v}_\mathrm{s} - \mathbf{v}) \rrbracket \cdot \mathbf{n} \tag{119}$$

Denoting the average $\langle\!\langle \cdot \rangle\!\rangle = \frac{1}{2}(\cdot_- + \cdot_+)$, the following product relationship may be derived: $\llbracket \mathbf{ab} \rrbracket = \llbracket \mathbf{a} \rrbracket\ \langle\!\langle \mathbf{b} \rangle\!\rangle + \langle\!\langle \mathbf{a} \rangle\!\rangle\ \llbracket \mathbf{b} \rrbracket$. Thus,

$$\begin{aligned} \llbracket \boldsymbol{\sigma}\, \mathbf{v}_\mathrm{s} \rrbracket \cdot \mathbf{n} &= \left(\llbracket \boldsymbol{\sigma} \rrbracket\ \langle\!\langle \mathbf{v}_\mathrm{s} \rangle\!\rangle + \langle\!\langle \boldsymbol{\sigma} \rangle\!\rangle\ \llbracket \mathbf{v}_\mathrm{s} \rrbracket\right) \cdot \mathbf{n} \\ &= \llbracket \boldsymbol{\sigma}\, \mathbf{n} \rrbracket \cdot \mathbf{v}_\mathrm{s} \\ &= \left(-\ \left\llbracket \rho \mathbf{v}\left(v_{\mathrm{s}_\mathrm{n}} - v_n\right)\right\rrbracket - \nabla_\mathrm{s}\ \cdot (\mathbf{P}\boldsymbol{\sigma}_\mathrm{s})\right) \cdot \mathbf{v}_\mathrm{s} \end{aligned} \tag{120}$$

where we have used Eqs. (23) and (111). Thus, using Eq. (93), and substituting Eqs. (120) into (119), we get:

$$\llbracket \boldsymbol{\sigma}\, \mathbf{v} \rrbracket \cdot \mathbf{n} = -\ \left\llbracket \rho \mathbf{v}_\mathrm{s} \cdot \mathbf{v}\left(v_{\mathrm{s}_\mathrm{n}} - v_n\right)\right\rrbracket - \llbracket \boldsymbol{\sigma}\ (\mathbf{v}_\mathrm{s} - \mathbf{v}) \rrbracket \cdot \mathbf{n} - (\nabla_\mathrm{s}\ \cdot (\mathbf{P}\boldsymbol{\sigma}_\mathrm{s})) \cdot \mathbf{v}_\mathrm{s} \tag{121}$$

F Derivation of the second law condition in the reference configuration

Writing $(\mathbf{v}_\mathrm{s} - \mathbf{v}) = \mathbf{F}\mathbf{V}_\mathrm{S}$, the second law condition Eq. (37) can be rewritten as,

$$\int_{\Gamma_\mathrm{s}} \mathbf{V}_\mathrm{S} \cdot \left\llbracket \mathbf{F}^\mathrm{T}\left(\rho\psi\mathbf{I} - \rho\sum_{\alpha=1}^{N}\mu^\alpha \nu^\alpha \mathbf{I} - \boldsymbol{\sigma}\right)\right\rrbracket \mathbf{n}\, \mathrm{d}\Gamma_\mathrm{s} \geq 0 \tag{122}$$

Nanson's formula [38] is now used to relate the differential surfaces in current and reference configurations,

$$\mathbf{n}\ \mathrm{d}\Gamma_\mathrm{s} = J\mathbf{G}^\mathrm{T}\mathbf{N}\ \mathrm{d}\Gamma_{\mathrm{s}_0} \tag{123}$$

where $J = det(\mathbf{F}) > 0$ is the Jacobian or the determinant of the deformation gradient $\mathbf{F}$, $\mathbf{G} = \mathbf{F}^{-1} = \frac{\partial \mathbf{X}}{\partial \mathbf{x}}$ is the inverse of the deformation gradient, and $\mathbf{N}$ is the normal to the interface in the reference configuration. By the definition of the first Piola–Kirchhoff stress tensor,

$$\int_{\Gamma_\mathrm{s}} \llbracket \boldsymbol{\sigma} \rrbracket\, \mathbf{n}\, \mathrm{d}\Gamma_\mathrm{s} = \int_{\Gamma_{\mathrm{s}_0}} \llbracket \boldsymbol{\sigma}_\mathrm{I} \rrbracket\, \mathbf{N}\, \mathrm{d}\Gamma_{\mathrm{s}_0} \tag{124}$$

leading to the expression

$$\boldsymbol{\sigma}_\mathrm{I} = J\boldsymbol{\sigma}\mathbf{G}^\mathrm{T} \tag{125}$$

Thus, expressing the integral in Eq. (122) in the reference configuration, and using the fact that $\mathit{\Gamma}_{\mathrm{s}_0}$ is arbitrary, we get the second law condition in reference configuration as

$$\mathbf{V}_\mathrm{S}\cdot\left[\!\!\left[\rho_0\left(\psi_0-\sum_{\alpha=1}^{N}\mu_0^\alpha\nu_0^\alpha\right)\mathbf{I}-\mathbf{F}^\mathrm{T}\boldsymbol{\sigma}_\mathrm{I}\right]\!\!\right]\mathbf{N}\geq 0 \quad \text{on} \;\; \mathit{\Gamma}_{\mathrm{s}_0} \tag{126}$$

Using the fact that the deformation gradient $\mathbf{F}=\frac{\partial\mathbf{x}}{\partial\mathbf{X}}=\mathbf{I}+\nabla_0\mathbf{U}^\mathrm{T}$ we can express the above condition in the following alternative form,

$$\mathbf{V}_\mathrm{S}\cdot\left[\!\!\left[\Sigma_0-\rho_0\sum_{\alpha=1}^{N}\mu_0^\alpha\nu_0^\alpha\mathbf{I}-\boldsymbol{\sigma}_\mathrm{I}\right]\!\!\right]\mathbf{N}\geq 0 \quad \text{on} \;\; \mathit{\Gamma}_{\mathrm{s}_0} \tag{127}$$

where we have used the fact that $\rho_0=J\rho$. $\Sigma_0=\rho_0\psi_0\mathbf{I}-\nabla_0\mathbf{U}\boldsymbol{\sigma}_\mathrm{I}$ is the Eshelby energy–momentum tensor [39] in the reference configuration.

References

1. Jones, D.R., Ashby, M.F.: Engineering Materials 2: An Introduction to Microstructures, Processing and Design. Butterworth-Heinemann, Oxford (2005)
2. Tarascon, J.M., Armand, M.: Issues and challenges facing rechargeable lithium batteries. Nature **414**(6861), 359–367 (2001)
3. Girishkumar, G., McCloskey, B., Luntz, A., Swanson, S., Wilcke, W.: Lithium–air battery: promise and challenges. J. Phys. Chem. Lett. **1**(14), 2193–2203 (2010)
4. Sunwoo, A., Morris, J., Lucey, G.: The growth of cu-sn intermetallics at a pretinned copper–solder interface. Metall. Trans. A **23**(4), 1323–1332 (1992)
5. Udupa, A., Sadasiva, S., Subbarayan, G.: A framework for studying dynamics and stability of diffusive–reactive interfaces with application to cu6sn5 intermetallic compound growth. Proc. R. Soc. Math. Phys. Eng. Sci. **472**, 20160134 (2016)
6. Amar, M.B., Goriely, A.: Growth and instability in elastic tissues. J. Mech. Phys. Solids **53**(10), 2284–2319 (2005)
7. Li, X., Magnuson, C.W., Venugopal, A., Tromp, R.M., Hannon, J.B., Vogel, E.M., Colombo, L., Ruoff, R.S.: Large-area graphene single crystals grown by low-pressure chemical vapor deposition of methane on copper. J. Am. Chem. Soc. **133**(9), 2816–2819 (2011)
8. Wang, W., Suo, Z.: Shape change of a pore in a stressed solid via surface diffusion motivated by surface and elastic energy variation. J. Mech. Phys. Solids **45**(5), 709–729 (1997)
9. Gleixner, R., Nix, W.: A physically based model of electromigration and stress-induced void formation in microelectronic interconnects. J. Appl. Phys. **86**(4), 1932–1944 (1999)
10. Sukharev, V., Zschech, E.: A model for electromigration-induced degradation mechanisms in dual-inlaid copper interconnects: effect of interface bonding strength. J. Appl. Phys. **96**(11), 6337–6343 (2004)
11. Xia, L., Bower, A.F., Suo, Z., Shih, C.: A finite element analysis of the motion and evolution of voids due to strain and electromigration induced surface diffusion. J. Mech. Phys. Solids **45**(9), 1473–1493 (1997)
12. Basaran, C., Lin, M., Ye, H.: A thermodynamic model for electrical current induced damage. Int. J. Solids Struct. **40**(26), 7315–7327 (2003)
13. Abeyaratne, R., Knowles, J.K.: On the driving traction acting on a surface of strain discontinuity in a continuum. J. Mech. Phys. Solids **38**(3), 345–360 (1990)
14. Fried, E., Gurtin, M.E.: Coherent solid-state phase transitions with atomic diffusion: a thermomechanical treatment. J. Stat. Phys. **95**(5–6), 1361–1427 (1999)
15. Gurtin, M.E.: Configurational Forces as Basic Concepts of Continuum Physics, vol. 137. Springer, Berlin (1999)
16. Lane, M., Liniger, E., Lloyd, J.: Relationship between interfacial adhesion and electromigration in cu metallization. J. Appl. Phys. **93**(3), 1417–1421 (2003)
17. Avrami, M.: Kinetics of phase change II. Transformation-time relations for random distribution of nuclei. J. Chem. Phys. **8**(2), 212–224 (1940)
18. Cahn, J.W.: The kinetics of grain boundary nucleated reactions. Acta Metall. **4**(5), 449–459 (1956)
19. Christian, J.W.: The Theory of Transformations in Metals and Alloys. Newnes, London (2002)
20. Kelton, K., Greer, A.: Nucleation in Condensed Matter: Applications in Materials and Biology. Pergamon Materials Series, vol. 15. Pergamon, Oxford (2010)
21. Shatzkes, M., Lloyd, J.: A model for conductor failure considering diffusion concurrently with electromigration resulting in a current exponent of 2. J. Appl. Phys. **59**(11), 3890–3893 (1986)
22. Lloyd, J., Kitchin, J.: The electromigration failure distribution: the fine-line case. J. Appl. Phys. **69**(4), 2117–2127 (1991)
23. Chao, B., Chae, S.H., Zhang, X., Lu, K.H., Ding, M., Im, J., Ho, P.S.: Electromigration enhanced intermetallic growth and void formation in pb-free solder joints. J. Appl. Phys. **100**(8), 084909 (2006)
24. Tu, K., Yeh, C., Liu, C., Chen, C.: Effect of current crowding on vacancy diffusion and void formation in electromigration. Appl. Phys. Lett. **76**(8), 988–990 (2000)
25. Yeh, E.C., Choi, W., Tu, K., Elenius, P., Balkan, H.: Current-crowding-induced electromigration failure in flip chip solder joints. Appl. Phys. Lett. **80**(4), 580–582 (2002)
26. Gleixner, R., Clemens, B., Nix, W.: Void nucleation in passivated interconnect lines: effects of site geometries, interfaces, and interface flaws. J. Mater. Res. **12**(08), 2081–2090 (1997)

27. Clement, J., Thompson, C.: Modeling electromigration-induced stress evolution in confined metal lines. J. Appl. Phys. **78**(2), 900–904 (1995)
28. Kirchheim, R.: Stress and electromigration in al-lines of integrated circuits. Acta Metall. Mater. **40**(2), 309–323 (1992)
29. Bower, A.F., Shankar, S.: A finite element model of electromigration induced void nucleation, growth and evolution in interconnects. Model. Simul. Mater. Sci. Eng. **15**(8), 923 (2007)
30. Xu, X.P., Needleman, A.: Void nucleation by inclusion debonding in a crystal matrix. Model. Simul. Mater. Sci. Eng. **1**(2), 111 (1993)
31. Bhandakkar, T.K., Gao, H.: Cohesive modeling of crack nucleation under diffusion induced stresses in a thin strip: implications on the critical size for flaw tolerant battery electrodes. Int. J. Solids Struct. **47**(10), 1424–1434 (2010)
32. Singh, N., Bower, A., Shankar, S.: A three-dimensional model of electromigration and stress induced void nucleation in interconnect structures. Model. Simul. Mater. Sci. Eng. **18**(6), 065006 (2010)
33. Basaran, C., Nie, S.: An irreversible thermodynamics theory for damage mechanics of solids. Int. J. Damage Mech. **13**(3), 205–223 (2004)
34. Yao, W., Basaran, C.: Computational damage mechanics of electromigration and thermomigration. J. Appl. Phys. **114**(10), 103708 (2013)
35. Clemens, B., Nix, W., Gleixner, R.: Void nucleation on a contaminated patch. J. Mater. Res. **12**(8), 2038–2042 (1997)
36. Truesdell, C., Toupin, R.: The classical field theories. In: Flügge, S. (ed.) Principles of Classical Mechanics and Field Theory/Prinzipien der Klassischen Mechanik und Feldtheorie, pp. 226–858. Springer, Berlin (1960)
37. Gurtin, M.E., Jabbour, M.E.: Interface evolution in three dimensions with curvature-dependent energy and surface diffusion: interface-controlled evolution, phase transitions, epitaxial growth of elastic films. Arch. Ration. Mech. Anal. **163**(3), 171–208 (2002)
38. Gurtin, M.E., Fried, E., Anand, L.: The Mechanics and Thermodynamics of Continua. Cambridge University Press, New York (2010)
39. Eshelby, J.: The elastic energy–momentum tensor. J. Elast. **5**(3–4), 321–335 (1975)
40. Rice, J.R.: A path independent integral and the approximate analysis of strain concentration by notches and cracks. J. Appl. Mech. **35**(2), 379–386 (1968)
41. Landau, L.D., Lifshitz, E.M.: Statistical Physics, 2nd edn. Addison-Wesley Pub. Co., Reading (1969)
42. Servi, I., Turnbull, D.: Thermodynamics and kinetics of precipitation in the copper–cobalt system. Acta Metall. **14**(2), 161–169 (1966)
43. LeGoues, F., Aaronson, H.: Influence of crystallography upon critical nucleus shapes and kinetics of homogeneous fcc–fcc nucleation. Comparisons between theory and experiment in cu–co alloys. Acta Metall. **32**(10), 1855–1864 (1984)
44. Volmer, M., Weber, A.: Keimbildung in übersättigten gebilden. Z. Phys. Chem. **119**, 277–301 (1926)
45. Turnbull, D., Fisher, J.C.: Rate of nucleation in condensed systems. J. Chem. Phys. **17**(1), 71–73 (1949)
46. Blech, I.A.: Electromigration in thin aluminum films on titanium nitride. J. Appl. Phys. **47**(4), 1203–1208 (1976)
47. Gurtin, M., Struthers, A., Williams, W.: A transport theorem for moving interfaces. Q. Appl. Math. **47**(4), 773–777 (1989)